ArcheoInt: An upgraded compilation of geomagnetic field intensity data for the past ten millennia and its application to the recovery of the past dipole moment

A. Genevey, Y Gallet, C. G Constable, M Korte, G G Hulot

Geochemistry Geophysics Geosystems G3
AN ELECTRONIC JOURNAL OF THE EARTH SCIENCES
Published by AGU and the Geochemical Society

Article
Volume 9, Number 4
29 April 2008
Q04038, doi:10.1029/2007GC001881
ISSN: 1525-2027

ArcheoInt: An upgraded compilation of geomagnetic field intensity data for the past ten millennia and its application to the recovery of the past dipole moment

A. Genevey
Centre de Recherche et de Restauration des Musées de France, UMR 171, CNRS, Palais du Louvre—Porte des Lions, 14 Quai François Mitterrand, F-75001 Paris, France (agnes.genevey@culture.gouv.fr)

Y. Gallet
Equipe de Paléomagnétisme, Institut de Physique du Globe de Paris, UMR 7154, CNRS, 4 Place Jussieu, F-75005 Paris, France (gallet@ipgp.jussieu.fr)

C. G. Constable
Institute for Geophysics and Planetary Physics, Scripps Institution of Oceanography, University of California, San Diego, 9500 Gilman Drive, La Jolla, California 92093-0225, USA (cconstable@ucsd.edu)

M. Korte
GeoForschungsZentrum Potsdam, Telegrafenberg, D-14473 Potsdam, Germany (monika@gfz-potsdam.de)

G. Hulot
Equipe de Géomagnétisme, Institut de Physique du Globe de Paris, UMR 7154, CNRS, 4 Place Jussieu, F-75005 Paris, France (gh@ipgp.jussieu.fr)

[1] This paper presents a compilation of intensity data covering the past 10 millennia (ArcheoInt). This compilation, which upgrades the one of Korte et al. (2005), contains 3648 data and incorporates additional intensity and directional data sets. A large majority of these data (~87%) were acquired on archeological artifacts, and the remaining ~13% correspond to data obtained from volcanic products. The present compilation also includes important metadata for evaluating the intensity data quality and providing a foundation to guide improved selection criteria. We show that ~50% of the data set fulfill reasonable reliability standards which take into account the anisotropic nature of most studied objects (potsherds), the stability of the magnetization, and the data dispersion. The temporal and geographical distributions of this sub–data set are similar to those of the main data set, with ~72% of the data dated from the past three millennia and ~76% obtained from western Eurasia. Approximately half of the selected intensity data are associated with at least an inclination value. To constrain the axial and full dipole evolution over the past three millennia requires that we avoid any overrepresentation of the western Eurasian data. We introduce a first-order regional weighting scheme based on the definition of eight widely distributed regions of 30° width within which the selected data are numerous enough. The regional curves of virtual axial dipole moments (VADM) and of mixed VADM-virtual dipole moments (VDM) averaged over sliding windows of 200 years and 500 years testify for strong contributions from either equatorial dipole or nondipole components. The computation of global VADM and mixed VADM/VDM variation curves, assuming an equal weight for each region, yields a dipole evolution marked by a distinct minimum around 0 B.C./A.D. followed by a maximum around the third-fourth century A.D. A second minimum is present around the eighth century A.D. This variation pattern is compatible with the one deduced from earlier, more

sophisticated analysis based on the inversion of both intensity and directional data. In particular, there is a good agreement among all VADMs and dipole moment estimates over the historical period, which further strengthens the validity of our weighting scheme.

Components: 14,277 words, 15 figures, 3 tables.

Keywords: data compilation; archeointensity; dipole evolution; Holocene; regional variations.

Index Terms: 1503 Geomagnetism and Paleomagnetism: Archeomagnetism; 1521 Geomagnetism and Paleomagnetism: Paleointensity; 1522 Geomagnetism and Paleomagnetism: Paleomagnetic secular variation.

Received 31 October 2007; **Revised** 23 January 2008; **Accepted** 6 February 2008; **Published** 29 April 2008.

Genevey, A., Y. Gallet, C. G. Constable, M. Korte, and G. Hulot (2008), ArcheoInt: An upgraded compilation of geomagnetic field intensity data for the past ten millennia and its application to the recovery of the past dipole moment, *Geochem. Geophys. Geosyst.*, *9*, Q04038, doi:10.1029/2007GC001881.

1. Introduction

[2] Global modeling of the Earth's magnetic field over the past few millennia requires the use of large compilations of both directional and intensity data. While the description of geomagnetic directional data usually is relatively straightforward, that of field intensity data is by contrast more complex. Knowledge of the age of the studied samples (as for directions), of the definition of a site and of the experimental procedures, including the corrections applied to account for the anisotropy of the thermoremanent magnetization (TRM) and for the cooling rate dependence of TRM acquisition, are all important parameters in evaluating paleointensity data. As a consequence, not all intensity data sets can be considered equivalently reliable and efforts toward geomagnetic field modeling must integrate that diversity through selection and/or ranking of the available data.

[3] *Korte et al.* [2005] recently built a compilation of directional and intensity data covering the past 7 ka (available from the EarthRef Digital Archive, ERDA). That compilation was intended for deriving global models, such as the CALS7K.2 model of *Korte and Constable* [2005a] and included a subset of data from the present work, which was still in progress at the time. *Korte et al.* [2005] made a consistent evaluation of the data through uncertainty estimates, but details like material, experimental procedure and corrections had not been listed with the data. The present paper should thus be viewed as an upgraded compilation of intensity data, spanning the past ten millennia and including previously lacking important metadata for evaluating the data quality. It follows, and in some way integrates, previous intensity compilations carried out by *McElhinny and Senanayake* [1982], *Burlatskaya et al.* [1986], *Yang et al.* [2000], *Korte et al.* [2005] and *Donadini et al.* [2006, 2007].

[4] The present upgraded compilation also incorporates additional data sets mainly acquired on lava flows from Hawaii, Italy and from the Canary Islands [e.g., *Tulloch*, 1992; *Laj et al.*, 2002]. It includes new information, in particular on technical aspects (i.e., experimental procedures, nature of the samples and meaning of the derived mean intensity values) whenever provided via personal conversations with the authors of reported studies. In particular, we acknowledge fruitful discussions with K. Burakov, S. Burtlatskaya and I. Nachasova, who obtained a large collection of intensity data from western Eurasia and several important modifications were made following instructions from these authors. Unlike *Korte et al.* [2005], who compiled intensity data independently from the directional data, we now simultaneously compile both directional and intensity data whenever they have been obtained from the same structures or objects making it possible to compute the VDM rather than just the VADM.

[5] In what follows we describe the general structure of the data tables and metadata compiled, before presenting statistics about the geographic and temporal distributions and about the various types of data. Then we turn to a discussion of experimental methods, providing a foundation to guide improved selection criteria when using data for regional and global analyses. The present compilation of geomagnetic field intensity data can be downloaded

1. Data table

	ArcheoInt_Number
	Short_Reference
Data Location and Provenance	Country
	Site
	Identification
	Lat
	Long
	ΔLat
	ΔLong
Material Description	Archeo/Volcanic
	In Place/Displaced
	Type_of_Material
	Sample_Form
Dating	Age_Method
	Age_Culture_Name
	C14_Lab_Number
	Age_description
	Age
	ΔAge
	Best_Age_Estimate
	ΔBest_Age_Estimate

Intensity Experimental Methods	**Method_Intensity**
	"pTRM-Check"_Test
	Correction_for_Alteration_Method
	Anisotropy_Correction_Method
	Cooling_Rate_Correction_Method
Statistical Information on the Mean Intensity Values	Nmean_INT
	Flag_INT
	NT_INT
	ns_INT
	INT
	ΔINT
	Def_ΔINT
	Authors_Intensity_Grade
Directional Information	Method_DIR
	Nmean_DIR
	Dec
	ΔDec
	Inc
	ΔInc
	k
	a95
VDMs and VADMs	VADM
	ΔVADM
	VDM
	ΔVDM

2. References table

Short_Reference	Short Reference of the paper(s)
Complete_Reference	Complete Reference of the paper(s)
Country(ies)	Country(ies) or Island(s)
N_Data	Number of intensity
Age_Min	Minimum Age of the data in "±years AD"
Age_Max	Maximum Age of the data in "±years AD"
Lat_Min	Minimum latitude of the data in decimal degrees
Lat_Max	Maximum latitude of the data in decimal degrees
Long_Min	Minimum longitude of the data in decimal degrees
Long_Max	Maximum longitude of the data in decimal degrees
Dir	Indicates whether or not directional information is available
Comments	Comments on the paper

3. Controlled vocabularies table

Abbreviations used in the ArcheoInt compilation	List of the abbreviations used with their corresponding explanation
Intensity Methods used in the ArcheoInt Compilation	List of the intensity methods used in the ArcheoInt compilation with the reference of the paper(s) where the methods are described
Controlled Vocabularies	Type of_Material
	Age_Method
	Method_Intensity
	"pTRM-check" Test
	Correction_for_Alteration_Method
	Anisotropy_Correction_Method
	Cooling_Rate_Correction_Method
	Def_ΔInt
	Method_DIR

4. Design table

Figure 1. Structure of the ArcheoInt compilation. The Excel worksheet includes four tables dealing primarily with (1) the data, (2) the references with additional details and remarks, (3) the abbreviations and the controlled vocabulary, and (4) the design of the data compilation. The bold font in the data table indicates the fields which are always documented for each intensity value.

from the ERDA web site (http://earthref.org/cgi-bin/er.cgi?s=erda.cgi?n=887).

2. Description of the Excel Workbook

[6] Our new compilation includes 3648 absolute intensity data, and these have been entered in an Excel workbook (ArcheoInt.xls). The basic format of the workbook resembles the one developed by *Perrin and Schnepp* [2004] for their 0–300 Ma paleointensity database version 2003, comprising 4 worksheets dealing primarily with (1) the data, (2) the references with additional details and remarks, (3) the abbreviations and the controlled vocabularies and (4) the design of the data compilation. This final table provides the definitions of the different fields documented in the three other tables. A simplified scheme of this sheet is shown in Figure 1. The general outline of each of the three other tables is described below.

2.1. Data Table

[7] The data table is the home for the actual intensity values themselves, but can contain numerous other fields that document their provenance and quality. These fields can be divided into seven main categories which we list here and describe in more detail in the ensuing sections 2.1.1–2.1.7: (1) data location and provenance, (2) material and sample description, (3) dating, (4) experimental methods, (5) intensity value and statistical information related to number of samples and inferred reliabil-

ity, (6) any associated directional data and information about their uncertainties, and (7) VADM and/or VDM results.

[8] Not every column of the data table is filled for any given result, because of the diversity of information recorded in the publications from which they are drawn. However, every intensity value entered in the data sheet is characterized by at least six different fields: (1) a record number which identifies the intensity datum in our compilation, (2) the (short) reference to the paper(s) where the data were presented, (3) the latitude, (4) longitude and (5) age of the studied structure(s) and (6) a generic description of the intensity method used by the authors. Except for the last field, the same information was given in the intensity data files described by *Korte et al.* [2005].

[9] It is also important to include more details about the intensity data, whenever available, in order to allow some judgment of individual data, independently from any, possibly quite subjective, uncertainty estimates. *Perrin and Schnepp* [2004] included some of these in their paleointensity database, but additional fields were defined in order to take into account specific methods used in archeointensity studies. In particular, this concerns the corrections for the TRM anisotropy and for cooling rate effects, which are usually not evaluated in classical paleointensity experiments. We did not intend to be exhaustive but tried to display characteristics that we believe are essential for the evaluation, ranking and/or the selection of the archeointensity data.

2.1.1. Data Location and Provenance

[10] In addition to the latitude and longitude, the first category includes two more fields providing the name of the country and the name of the site where the samples were collected. Another column, so-called "identification," is used for entering the label chosen by the authors to identify their intensity data. In many cases, this label is a laboratory or an arbitrary number, but in other instances it corresponds to an archeological tag on a monument, a stratigraphic unit or to the name of a volcanic outcrop, all of which therefore provides additional information on the location. It should be pointed out that the precise location of the studied objects or structures was not systematically given by the authors. When the name of a city, an archeological site or a volcano was indicated in the papers, a precise latitude and longitude for the data could often be recovered. But for some papers, the only information available was the name of a region or a country. A bounding box was then defined for the area of study. The mean latitude and longitude of this box were allocated to the data and uncertainties about this mean location defined in terms of the geographical extension of the box (ΔLat, ΔLong fields). Note also that for samples obtained from displaced archeological artifacts (i.e., displaced from the location of their initial baking) the place where the samples have been found is not always the relevant one for geomagnetic studies. Ceramics are good examples of such samples since production centers may sometimes be very distant from the places where potsherds are later discovered.

2.1.2. Material and Sample Description

[11] The material studied for the intensity determinations is documented in the present compilation with three columns providing the volcanic or archeological nature of the objects, their "in place" or "displaced" characteristic relative to the location of their last heating-cooling and their lithology or archeological classification. In addition, a final field displays a short description of the samples analyzed with indications on their form, size and the possible use of substance (like plaster) to embed the fragments.

2.1.3. Dating

[12] Dating, precision and reliability are key parameters in archeointensity studies. In our compilation, different fields define the method(s) used to constrain the age (Age_Method column) and, when specified in the papers, the name of the culture/dynasty/period associated with the analyzed archeological material (Age_Culture_Name column). This last information ensures a relative and independent dating of the samples and leaves room for future reevaluation of say the age of a culture. For some data, the ages were ascertained by radiocarbon dating and a calibration of the conventional C14 age was therefore necessary to account for the fluctuations of atmospheric C14. When a conventional age C14 was indicated in the original papers (or when we were able to find this age in the literature), a calibration using the calib4_3 software was systematically performed with the same settings as used by *Korte et al.* [2005], the 1998 atmospheric decadal variation curve being smoothed with a moving average over 5 points. No other correction or assumption was considered except for one C14 age obtained on a marine shell from the Japanese sea for which a

correction of the reservoir effect was necessary [*Kitazawa*, 1970]. Note that when two or more conventional C14 ages were associated to a single intensity value, a weighted C14 conventional age was computed for the calibration [*Bevington*, 1969] and the 95% confidence interval obtained from the probability distribution method was used to infer a mean calibrated age and its error.

[13] Both conventional and calibrated C14 ages have been included in our compilation. The conventional age is indeed the original information and providing it makes it possible for users to perform their own calibration. However, for comparison with other intensity data, only the calibrated age is relevant. The conventional C14 ages and standard deviations have thus been reported in the Age and ΔAge columns, while the calibrated ages and their uncertainty are entered in the Best_Age_Estimate and ΔBest_Age_Estimate columns. It is important to specify that the ages are given in "±years A.D.," negative years corresponding to years before Christ. To obtain ages in years before present (years B.P.), which is the standard unit used for conventional C14 ages, one may simply subtract the ages in "±years A.D." unit from 1950. When available, the radiocarbon laboratory number, identifying the radiocarbon laboratory where the measurements were obtained and the sample analyzed in that particular laboratory, was also entered in the present compilation. For some data, we were unable to reperform a calibration because only the calibrated ages were indicated in the papers. In these cases, the same ages were entered in both the Age and Best_Age_Estimate columns, but the exact definition of these two ages was systematically given in the Age_Description column. This column, which is particularly important for C14 ages, may also display other details on the age or on the dating method, for example when the ages were indicated as approximate or uncertain by the authors themselves.

[14] For some intensity results not dated by radiocarbon measurements, different ages (or no age at all) were sometimes entered in the Age and the Best_Age_Estimate columns. This was the case when new information was found in more recent papers, also quoted in our compilation, after, e.g., a temporal recalibration of a relative chronology. In most cases, however, the Age and the Best_Age_Estimate were simply set equal.

[15] In their previous compilation, *Korte et al.* [2005] assigned their own default age uncertainties when the latter were not indicated by the authors in the original papers. These estimates were indeed necessary for the computations of global geomagnetic field models [*Korte and Constable*, 2005a]. In the present compilation, no such default age uncertainties are reported to keep with the original information provided by the authors. Note, however, that for the computations of VADM/VDM curves, we did of course assign age uncertainties (see section 6).

2.1.4. Intensity Experimental Methods

[16] The third field category was defined to allow for a relatively detailed presentation of the intensity experiments used by the authors to obtain their data. The general description of the methods is provided via generic names (Thellier and Thellier, Shaw, Microwave,. . .). This information is complemented by four fields specifying (1) the use or not of pTRM-check test (for partial Thermoremanent Magnetization checks) when a Thellier derived protocol was applied (note that the boundary limit considered by the authors for a positive check is indicated when specified in the original papers), (2) the possible use of correction for alteration, (3) the correction for TRM anisotropy, and (4) the correction for the cooling rate TRM dependence effect. Note that although new tests and intensity protocols have recently been developed to detect multidomain (MD) grains behavior which could bias the intensity determination [e.g., *Dunlop and Ozdemir*, 1997; *Riisager and Riisager*, 2001; *Krasa et al.*, 2003; *Yu et al.*, 2004; *Leonhardt et al.*, 2004], this information is not provided in the present compilation as it concerns a very limited fraction (less than 1%) of the available intensity data.

2.1.5. Statistical Information on the Mean Intensity Values

[17] In this field category statistical parameters on each mean intensity result are reported, such as the error associated with the mean value, the definition of this error and the number of individual intensity values used to derive the mean. This rapid and simple description, however, hides some considerable complexity related to the diversity of the analyzed structures or objects, the variability of the site definition and the different methods used to compute the mean intensity values and their error bars.

[18] Each mean intensity result incorporated in our compilation corresponds to the data obtained for a dated site as indicated in the original publication. The definition of a site is, however, variable in archeomagnetic studies. When working on struc-

tures in place, such as a baked hearth, a kiln or a volcanic outcrop, the definition of a site is straightforward: the structure is considered as one site and the mean intensity is derived from intensity values obtained from different samples taken from this structure. But a very large number of archeointensity data were also obtained from small displaced archeological artifacts such as fragments of ceramics, tiles or baked bricks. In this case, the site may be either a single fragment or a set of different fragments dated of the same age. Both definitions were considered in the literature. Our philosophy was to enter in each case what was judged by the authors as the best estimate of the ancient geomagnetic field intensity. This approach was principally guided by arguments related to the temporal homogeneity of the fragments that may constitute a site. This temporal homogeneity is not systematically ensured for fragments found in the same archeological layer and dated within the same time interval. When the authors only gave intensity values at the fragment level in the original publications, we did not compute a mean intensity thus allowing for the possibility that the fragments could have been produced at different instants within their interval of age uncertainty. Conversely, when an average was computed by the authors, only this mean has been reported, and not the individual values, because we assumed that the authors considered the former mean value as the best estimate of the geomagnetic field intensity. This strategy is probably different from the one used by *Yang et al.* [2000]. The number of data included in their compilation is indeed close to the number of results in our own compilation although we entered new data sets. Moreover, when only considering the papers reported by *Yang et al.* [2000], we find a much lower number of intensity results, which indicates that they probably entered the data at the fragment level. Our approach, however, appears to be the same as the one followed by *McElhinny and Senanayake* [1982] and *Donadini et al.* [2006, 2007].

[19] In the present compilation, the number of data considered by the authors to derive a mean intensity value is indicated in the "Nmean_INT" column. This parameter can, however, have different meanings. It can correspond to the number of samples collected from a single thermal unit (i.e., a large structure still in place or a small displaced fragment) or to the number of samples collected from several thermal units dated of the same age (fragments from different pottery). To discriminate between these two cases, we introduced (in addition to the column specifying the type of material analyzed by the authors) two columns respectively providing the number "NT_INT" of studied thermal units and the total number "ns_INT" of samples analyzed and retained to compute the mean for this (these) thermal unit(s). For example, if an intensity mean value was derived from two values obtained from two samples taken from a same potsherd, NT_INT was then set to unity and ns_Int to 2 (Nmean_INT is 2). If the number of studied potsherds was 3 but with 2 samples per fragment, NT_INT was then set to 3 and ns_Int to 6. Note that in this case, Nmean_INT could be either 3 or 6 depending on the way the authors computed their mean. Another typical example is the case of a structure found in place, such as a kiln, from which three fragments of bricks (taken from the kiln) have been analyzed for intensity. The site is then the oven and the different bricks, samples from this kiln, which hence acquired their magnetization at the same time during the last cooling of the structure. In this case, NT_INT would be set to 1 and ns_Int to 3. In several studies, however, there was an ambiguity with respect to the number of intensity values used to derive the means and we were unable to determine if the "N" indicated by the authors was the number of samples from a single fragment or the number of different fragments (with probably a combination of both possibilities in some cases). Note that we then usually chose the second and in a way more "optimistic" option, underlying this ambiguity by a star in the "Flag_Int" column.

[20] Various options were also used by the authors to report the precision associated with each mean intensity data. We tried to standardize these errors and chose to enter a standard deviation among the individual intensity values whenever possible. This standard deviation was sometimes recomputed from the standard error indicated in the original papers. However, in several cases, we were not able to associate a standard deviation to an intensity value because of a lack of information or proper definition in the original publications. In those cases, we nevertheless reported the errors provided by the authors in the "error column" and indicated their definition in the corresponding column (Def_ΔInt).

[21] The final column in this field category displays the reliability of the data as graded by the authors themselves. Several parameters were considered for that ranking. The grades for the data set acquired by *Aitken et al.* [1984, 1988a, 1988b,

1989a, 1989b, 1991] [see also *Wei et al.*, 1987; *Papamarinopoulos*, 1987] were directly linked to the dispersion, expressed in percentage, of the intensity values obtained from samples of a same site. But in most other cases, the ranking was not based on statistical factors related to the mean intensity values and relied on other parameters, sometimes more subjective, such as the visual scattering in intensity diagrams.

2.1.6. Directional Information

[22] The upgraded intensity compilation also includes directional information whenever both intensity and directional data were obtained from the same objects or structures. This new information is reported in different columns which detail the method used for these determinations, the number of analyzed samples, the declination (when determined), the inclination and the associated errors. The errors can be on the inclination only and is then provided as a standard deviation around the mean inclination value, or on both the declination and the inclination. To account for the fact that these errors may have been computed separately by the authors, these are entered again as standard deviations in two columns unless an "$\alpha 95$" [*Fisher*, 1953] was indicated by the authors which we then reported in the corresponding column. Another column displays the Fisher parameter k when provided in the papers.

2.1.7. VADMs and VDMs

[23] The location and directional information can be used to produce two additional fields, one for the VADM computed from the data and the other for the VDM when inclinations were provided. These values and their uncertainties (whenever possible) were computed from the following formulas [e.g., *Merrill et al.*, 1996]:

$$VADM = \frac{4\pi R^3 F}{\mu_0 \left(1 + 3\sin^2 \lambda\right)^{0.5}}$$

$$VDM = \frac{4\pi R^3 F (1 + 3\cos^2 Inc)^{0.5}}{2\mu_0}$$

with μ_0 the permeability of free space ($\mu_0 = 4\pi 10^{-7}$ H.m^{-1}), R the radius of the Earth (R = 6371 km), F the intensity in micro Telsa, λ the latitude of the site in degree, and Inc the inclination associated to the intensity in degree.

2.2. Table of References

[24] The reference table provides all the complete references of the papers included in the present compilation. Important information on each publication is also reported in this table, such as the age window, the geographical bounding box of each study, the names of the country(ies) where the samples were collected and the number of intensity results reported. A comment field further makes it possible to specify when intensity data not reported in a table, had nevertheless been recovered from a figure (by scanning the figures). This field also includes some comments regarding the ages of the data, the location of the sampling sites, the definition of these sites and how the mean intensity values were obtained (in particular with possible weighting).

2.3. Controlled Vocabularies

[25] When building this compilation, the main objective was to make it as intuitive as possible for the users. Abbreviations are therefore rare and restricted to those very common for paleomagnetic studies. Codes for the different fields were also defined to be most straightforward.

[26] The third table of the ArcheoInt compilation defines the few abbreviations employed and lists the selected terms for each main category of metadata. For the intensity methods, we further indicated the reference of the paper(s) where the protocols were first defined and/or fully described.

3. Type, Geographic, and Temporal Distribution of the Data

[27] Approximately 87% of the intensity data reported in the present compilation were acquired on archeological artifacts, while the remaining ~13% correspond to data obtained from volcanic products. The latter proportion is slightly higher than the one in *Korte et al.* [2005] because the newly entered data were mostly obtained from lava flows. Among the archeological data, those acquired on displaced artifacts are predominant, corresponding to ~66% of the results, and ~57% if the whole (archeological and volcanic) data set is considered. Data obtained from structures found in situ represent ~21.5% of the archeological data set and the last ~12.5% include archeological structures or objects that were not clearly specified in the original publications.

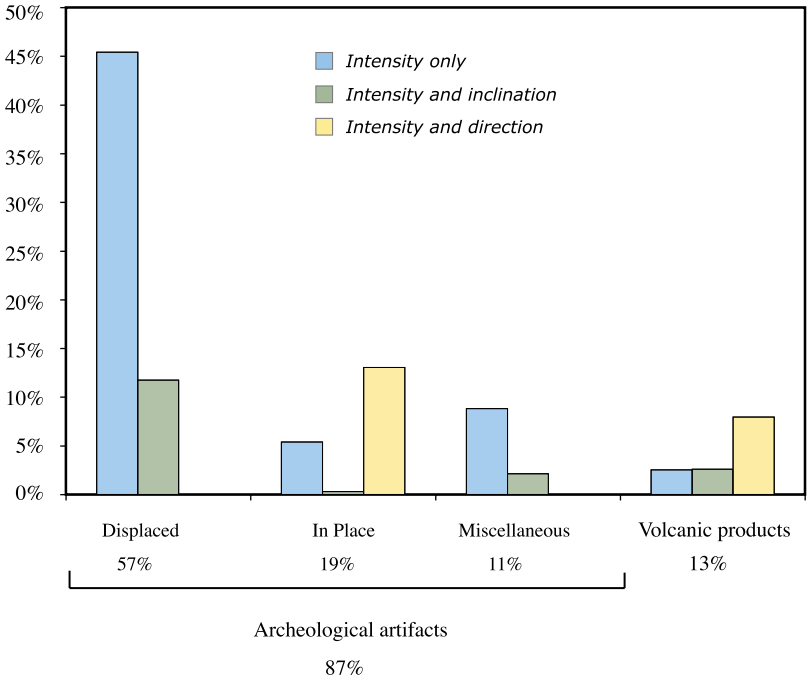

Figure 2. Proportions of intensity data acquired alone (in blue) or associated with directional information (green, inclinations only; yellow, both declinations and inclinations) as a function of type of analyzed objects. "Miscellaneous" includes archeological artifacts of unknown type.

[28] Directional information is available for only ~38% of the whole data set (Figure 2). This reflects the fact that intensity experiments were principally carried out on displaced archeological artifacts. For ~20% of these objects, geomagnetic inclinations were, however, determined. These are mainly bricks for which two hypotheses had to be made with respect to their baking position in the oven: first, that the oven floor or the surface where the bricks were placed during the firing had been horizontal and second, that the bricks themselves had been positioned lying on one of their flat sides.

[29] The intensity data are not evenly distributed over the globe (Figure 3). Only ~5% of the data are from the southern hemisphere and among this small proportion, ~74% were obtained from Peru. The southern hemisphere is thus almost devoid of data. The situation is better for the northern hemisphere although the distribution of the data is far from ideal, as nearly 70% of the intensity data are

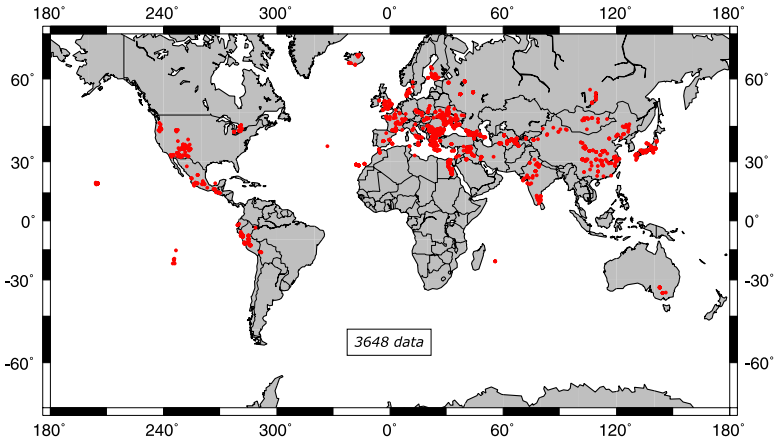

Figure 3. Geographical distribution of the intensity data (red dots) provided in the present ArcheoInt compilation.

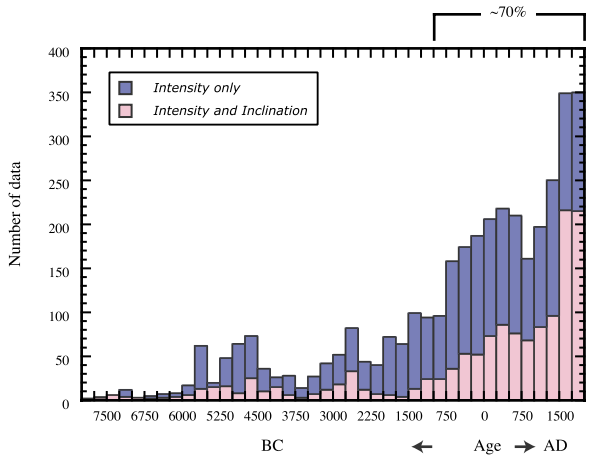

Figure 4. Temporal distribution using 250-year bins of the intensity data provided in the present ArcheoInt compilation (blue, intensity data only; pink, intensity data with inclination).

clustered in the western Eurasian area. The rest of the data was essentially obtained in eastern Asia (∼12%), in the southwest part of the North America (∼6%) and in Hawaii (∼5%).

[30] The temporal distribution of the available intensity data is also clearly nonuniform with about 70% of the results dated from the past three millennia (Figure 4). The dating constraints are not systematically specified in the papers, and for ∼49% of the objects analyzed they are linked to archeological arguments, including stratigraphy and/or relative chronology of human societies. About 7% of the results were dated on the basis of historical events, mainly well-known volcanic eruptions. The radiocarbon method was rarely used alone (∼6.5% of the data set), but often combined with other methods. About 20% of the intensity data had their age determined using a combination of different types of constraints (archeomagnetism, radiocarbon, thermoluminescence, dendrochronology, archeology, etc.).

4. Diversity of the Experimental Methods

[31] Most of the data (about 90%) were obtained by thermal demagnetization of the Natural Remanent Magnetization (NRM) recorded by the objects during their last cooling following the methodology developed either by *Thellier and Thellier* [1959] or *Wilson* [1961]. More precisely, ∼51% of the whole data set were acquired by relying on the original *Thellier and Thellier* [1959] method via a double heating-cooling cycle performed in field, while ∼22% relied on the *Coe* [1967] version of the Thellier and Thellier method (i.e., double heating-cooling step performed first in zero field and then in field) and ∼9% relied on the Aitken [e.g., *Aitken et al.*, 1988a] version of the method (i.e., double heating-cooling step performed first in field, then in zero field).

[32] Another ∼6% of the data were acquired by relying on methods based on NRM demagnetization in alternating fields as developed by *Shaw* [1974] and *Van Zijl et al.* [1962]. For the remaining data, microwave demagnetization technique (∼2.5% of the data [*Walton et al.*, 1993]), combined protocols (∼0.5%) and an adapted version of the *Shaw* [1974] method applied to adobe bricks for which the magnetization acquisition is due to a shear strain induced by the molding of the humid clay (41 absolute intensity data acquired by *Games* [1977, 1980]) were used.

[33] The categorization above does not completely reflect the diversity of the protocols used by the authors. One critical parameter concerns the control of alteration of the magnetic mineralogy during the experiments. pTRM-check tests, first introduced by *Thellier and Thellier* [1959], which give an estimate of the stability of the TRM acquisition capacity, are widely considered as the most efficient methods for detecting magnetic alteration during thermal treatment and are now requested to constrain the reliability of intensity results. No such tests, however, were performed for ∼52% of the relevant data (i.e., that acquired using a Thellier and Thellier type protocol with a thermal or a microwave demagnetization), most of which were acquired before 1985. After 1985 indeed these checks were more systematically included in the experimental routine. But even when used, the pTRM-check tests were not all equivalent, with differences in the way the percentage of alteration was computed (difference ratio normalized either by the pTRM, the total TRM or by the hypotenuse of the selected segment, i.e., using the so-called DRAT introduced by *Selkin and Tauxe* [2000]), the number of tests performed, the threshold value (not systematically indicated by the authors), the number of samples for which the tests were made (in some studies, checks were only performed for a part of the collection), etc.

[34] Several authors tried to correct their intensity values for the effect of alteration detected during the thermal treatment. About 50% of the data acquired using the Shaw-type methods were for

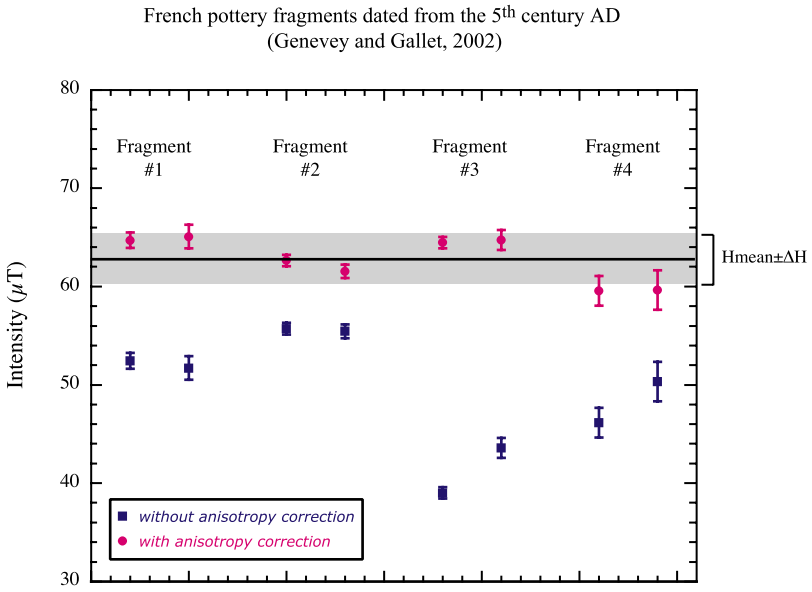

Figure 5. Example of TRM anisotropy effect on French ceramic fragments (site A29 [*Genevey and Gallet*, 2002]). The two specimens analyzed per fragment were oriented along the same direction relative to that of the applied laboratory field. Intensity results before (after) TRM anisotropy correction are indicated in blue (pink) after cooling rate correction. The shaded band shows the mean intensity value and its standard deviation obtained for this site.

instance corrected for alteration using factors based on measurements of the anhysteretic remanent magnetization [*Kono*, 1978; *Rolph and Shaw*, 1985]. But *Tanguy* [1975], *Burakov and Nachasova* [1985], *Walton* [1984, 1986, 1990], *Walton and Balhatchet* [1988] and more recently *Valet et al.* [1996] also developed correction methods applicable to the Thellier and Thellier or Wilson protocols. These corrections were applied to ~18% of the whole data set, mainly (~13%) using the *Burakov and Nachasova* [1985] correction method.

[35] A second key parameter is related to the anisotropy of the thermoremanent magnetization which can have a large effect on the intensity determinations, as can be seen in Figure 5. The TRM anisotropy observed in baked clay artifacts is generally interpreted as reflecting a preferential alignment of magnetic grains caused by a stretching of clay during the manufacturing process [e.g., *Rogers et al.*, 1979; *Aitken et al.*, 1981]. However, the TRM anisotropy effect was not investigated at all for 50% of the whole collection. For the second half, various approaches were considered to account for this parameter. For ~15% of the data, the field during laboratory TRM acquisition was applied in the direction of the NRM; a reasonable way to proceed if the anisotropy is weak enough. For strong anisotropic specimens, this approach is not adequate (unless of course the ancient field was parallel to one of the principal axes of the TRM tensor). *Aitken et al.* [1984, 1988a, 1988b, 1989a, 1989b, 1991; see also *Wei et al.*, 1987; *Papamarinopoulos*, 1987] therefore determined the TRM anisotropy tensor and corrected their intensity values whenever the angle between the TRM and the laboratory field directions was found to be large. Similarly, *Gallet et al.* [2006] [following *Le Goff and Gallet*, 2004] adjusted the direction of the laboratory field to always produce a TRM almost parallel to the NRM. In other cases the TRM anisotropy effect was evaluated directly through the determination of the TRM anisotropy tensor (~7.5%) or from other magnetic anisotropies, such as that of the magnetic susceptibility (MS; ~4.5%), of the isothermal remanent magnetization (IRM; ~8%) or of the anhysteretic magnetization (ARM, less than 1%). The remaining ~15% include data for which anisotropy was assumed negligible or for which anisotropy corrections were made using relationships experimentally established between the TRM and the MS or ARM anisotropy tensors. In particular, ~13% of the whole data set were corrected using the original procedure developed by *Burakov* [1981] involving the determination of parameters relating the TRM (and NRM) and susceptibility anisotropy tensors at several temperatures steps.

[36] Another important characteristic of the intensity procedures documented in our compilation concerns the cooling rate (CR) dependence of TRM

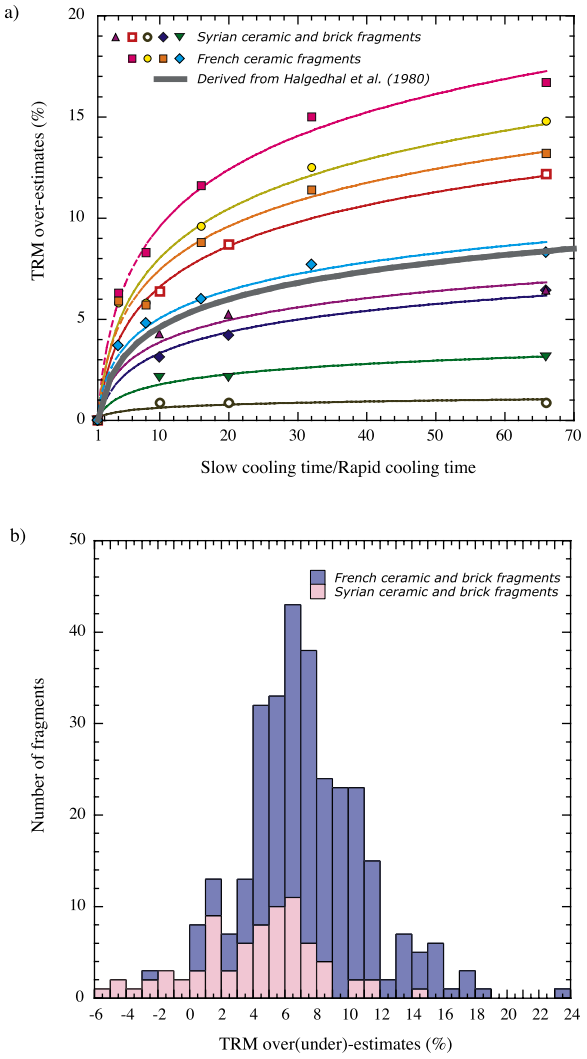

Figure 6. Cooling rate dependence of TRM acquisition. (a) Examples of evolution of the TRM overestimates obtained from several French and Syrian fragments of ceramics and bricks as a function of the ratio between different slow cooling durations (from 0.5 to 33 hours) and a fixed rapid (0.5 hour) cooling duration [*Genevey and Gallet*, 2002; *Genevey et al.*, 2003]. The thick line corresponds to the TRM overestimate derived from equation (11) of *Halgedhal et al.* [1980] for grains with a narrow blocking temperature range near the Curie temperature. (b) Histograms of the TRM overestimates (underestimates) obtained from a large collection of French and Syrian baked clay fragments [*Genevey and Gallet*, 2002; *Genevey et al.*, 2003] (and new data).

acquisition. This effect is predicted by Néel's theory [*Néel*, 1955; see also *Dodson and McClelland-Brown*, 1980; *Halgedahl et al.*, 1980] for single domain grain assemblages. It was further studied for different types of domain grains and experimentally observed for both volcanic products and archeological artifacts [e.g., *Fox and Aitken*, 1980; *Biquand*, 1994; *Chauvin et al.*, 2000; *Leonhardt et al.*, 2006]. This cooling rate effect is due to the fact that the cooling of the samples in the laboratory is typically faster than the original cooling. When not corrected, it usually results in overestimates for the intensity values, sometimes by more than 10% (Figure 6) [e.g., *Genevey and Gallet*, 2002]. For almost 80% of the data, no attempt was made, however, to evaluate this effect. Among the remaining ~20% fraction, the cooling rate effect was directly measured through additional experiments for ~40% of the data. The results of these studies were used by several authors to derive a rough estimate for a "reasonable" CR correction ("educated guess") which was then applied to ~14% of the CR corrected data. Some authors also judged that a CR correction was unnecessary in their study because the experimental and the original cooling rates were considered similar; this concerns ~29% of the collection of CR checked data. For an additional ~14% of this data, theoretical computations were made to derive a CR correction factor [*Walton*, 1984, 1990; *Walton and Balhatchet*, 1988]. Finally, we should also mention the case of archeointensity data recently acquired from high-temperature magnetization measurements [*Le Goff and Gallet*, 2004]. Those data represent ~3% of the CR corrected data [*Gallet and Le Goff*, 2006; *Gallet et al.*, 2006] for which the cooling rate effect was shown to be automatically corrected when using the experimental procedure developed by these authors.

[37] Although, as just emphasized, intensity protocols vary substantially among the 151 studies considered in this compilation, a few large homogeneous sub–data sets can still be identified. The most important one was acquired by K. Burakov and I. Nachasova after 1986. These data represent ~13% of the whole data set and were obtained using a procedure derived from the *Thellier and Thellier* [1959] method, including both corrections for the anisotropy effect [*Burakov*, 1981] and for the magnetic alteration during the thermal treatment [*Burakov and Nachasova*, 1985]. Before 1986, these authors mainly applied the original Thellier and Thellier method with pTRM-check and a limit of 10% for this alteration test (211 data, ~6%). The same protocol was also used by S. Burlatskaya and coauthors leading to a collection of 417 results (11% of the whole data set). Altogether, these authors from the Institute of Physics of the Earth (Russia Academy of Sciences)

acquired more than 30% of the archeointensity data included in our compilation. Of interest is the fact that they used pTRM-checks during their intensity experiments, although no indication on this important point was provided in the original publications (K. Burakov, S. Burlatskaya, and I. Nachasova, personal communication, 2004). The data of Aitken and coauthors also constitute another, yet smaller, homogenous collection of results (~6.5%), obtained using the ''In field-Zero Field'' version of the Thellier and Thellier method, with both corrections for anisotropy and cooling rate effects. Finally, one should also mention the important set of Bulgarian results (292 data, ~8%) obtained by *Kovacheva* [1997], who relied on the original Thellier and Thellier method, used pTRM-check tests after ~1982 and applied anisotropy correction using IRM anisotropy tensor after the eighties.

5. Discussion on Selection Criteria and Application to the Data Compilation

[38] The various intensity experiments and definitions of intensity sites considered by the authors clearly show that the data cannot be regarded as equally reliable. The definition (and the use) of criteria for selecting what one could judge as the ''best data'' is therefore a crucial issue, but not a simple task. Two approaches can be followed. The first consists in retaining all available data and weighting them according to some assigned measure of quality (or reliability). This is the approach chosen by *Korte and Constable* [2005a] for the computation of global geomagnetic field models. The second, alternative, approach is more selective and consists in eliminating those intensity data which do not fulfill minimal reliability standards. We explore below the consequences of such a strategy for our data set.

[39] First, consider standard basic criteria for selecting the data: (1) the data must be acquired using the original or derived Thellier and Thellier method with pTRM-check tests or with the Shaw procedure (here we ignore data obtained with correction for alteration), (2) the mean intensity value must be computed from at least three results, regardless of the definition of the site (fragment or group of fragments), (3) the standard deviation must be less than 15%, and (4) the TRM anisotropy effect must be taken into account for objects generally recognized as strongly anisotropic, such as fragments of pottery or tiles. Using these simple rather weak criteria would then lead us to select only 644 data, i.e., 18% of the whole data set, with no cooling rate correction for 543 of them. Most of the discarded data (~90%) would be rejected on the basis of criteria 1 and 2. Among the 644 retained results, 250 data were obtained from Bulgaria by M. Kovacheva with pTRM-checks performed only after ~1982 and another 135 data had either no threshold value indicated for the pTRM-check tests, or pTRM-checks only applied to part of the sample collection. Note that if more severe selection criteria were to be used, such as those normally favored: thermal method with pTRM-checks, anisotropy correction performed for all samples and quantified from the TRM anisotropy tensor (and not from a proxy, which is known to be a questionable approach [e.g., *Chauvin et al.*, 2000]), the final world data compilation would dramatically shrink to about 110 data.

[40] The four selection criteria above lead to the rejection of all data acquired with no pTRM-check, including those obtained by Aitken et al. and by Burakov and Nachasova after 1986. In that case, however, alternative strict criteria had been used by the authors and rejecting these data is therefore perhaps too severe. Aitken et al. applied strict criteria to keep only the most reliable data (grade 1, 2 and 3T [*Aitken et al.*, 1986, 1989a]) replacing the pTRM-check by a test on the linearity of the slope in their intensity diagrams. Only the results with an uncertainty of less than $(2/\sqrt{N-2})\%$ in the slope determination, N being the number of steps for this computation, were retained. As noted by Aitken et al., this stringent requirement indeed likely eliminates samples that suffered magnetic alteration during the thermal treatment. Moreover, data from Aitken et al. and from Burakov and Nachasova are generally very consistent with other results obtained with pTRM-check tests. This is for instance the case for data obtained from the Middle East and from Central Asia [*Nachasova and Burakov*, 2000; *Genevey et al.*, 2003; *Gallet et al.*, 2006]. In fact intercomparisons between data obtained by K. Burakov and I. Nachasova using their original protocol and data obtained using a more classical procedure [*Genevey and Gallet*, 2002] including pTRM-check, anisotropy correction via the determination of the TRM anisotropy tensor and cooling rate correction, show very consistent results. These intercomparisons (not yet published) were performed on brother specimens from C2RMF & IPGP's French and Syrian collection. This underlines the quality of the experimental work conducted by Burakov and Nachasova, validates their protocol and suggests that an alternative approach

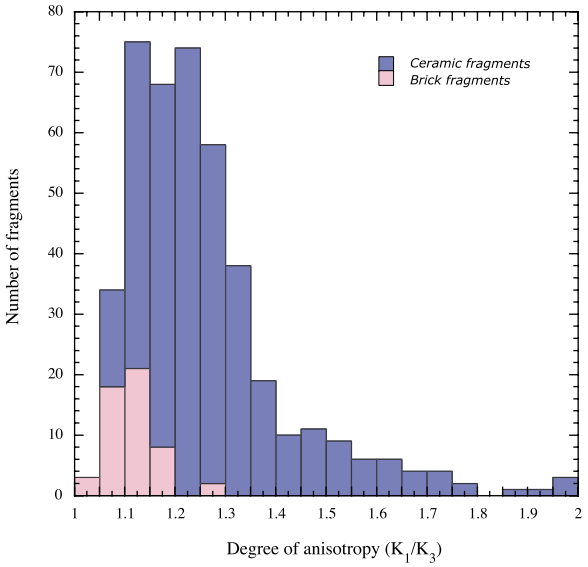

Figure 7. Histograms of the degree of TRM anisotropy measured on a large collection of French and Syrian fragments of ceramics and bricks [*Genevey and Gallet*, 2002; *Genevey et al.*, 2003] (and new data).

for assessing the reliability of the intensity compilation should be considered.

[41] A reasonable option would consist in compensating for the lack of pTRM-check tests for magnetic alteration by using other criteria based on the dispersion of the data about their mean intensity value as well as the number of samples analyzed per site. Indeed, if this number is sufficient and the dispersion low enough, one can hope that the magnetic alteration (if any) remained limited. The same approach could also be used for TRM anisotropy correction when dealing with anisotropic objects. Working along those lines, we defined several alternative selection criteria according to the type of the structure analyzed and to the characteristics of the intensity procedure, requesting the number of samples per object or the number of objects studied to be greater than two or three (depending on the protocol applied) with a dispersion around the mean no greater than 15%. In particular, we distinguished studied objects on the basis of their potential anisotropy. Figure 7 shows the degree of TRM anisotropy measured on a collection of 375 ceramic fragments analyzed in IPGP's laboratory [*Genevey and Gallet*, 2002; *Genevey et al.*, 2003] (and new data). It is obvious that for such fragments the anisotropy degree greatly varies between potsherds. This can strongly bias an intensity determination if not corrected for. By contrast, the degree of anisotropy observed in bricks is generally more limited (also shown in Figure 7). For selecting the data, we therefore suggest considering bricks as essentially isotropic. The same reasonable assumption can be made for the in place structures of volcanic (pyroclastic or lava flow) or archeological (kilns, ovens, hearth. . .) nature. In the case of potsherds and tiles for which neither pTRM-check nor anisotropy correction have been performed, the new criteria would consist in requiring a minimum of three different fragments analyzed per site to produce a mean intensity value. Indeed when working on a single fragment but with several studied specimens, one can obtain consistent intensity values if the specimens are roughly oriented along the same direction relative to that of the applied laboratory field. But, this consistency can also occur in the presence of strong TRM anisotropy and therefore be misleading (Figure 5). The analysis of several independent fragments is thus necessary to estimate the importance of the anisotropy effect when not experimentally corrected for.

[42] Tentatively applying this set of new criteria to our main database leads to a collection of 1839 data, i.e., ~50% of the whole data set, which fulfill quite minimal reliability standards. The characteristics of this sub–data set, i.e., the proportion of the different types of analyzed objects and their temporal and geographical distributions, are similar to those of the main database: ~72% of the selected data are dated from the past 3 millennia and ~76% were obtained from western Eurasia. The data are even more localized with ~54% confined inside a small geographical box of 30° in latitude and longitude centered around a mid point at 45° in latitude and 35° in longitude. The proportion of data with directional information is notably higher with ~47% of the results (instead of ~38% in the main database) associated with at least inclinations. This latter point is simply due to the fact that our selection criteria tend to reject anisotropic objects like pottery and tile fragments for which no directional information is usually available.

[43] The selection of the data discussed in this paragraph could be viewed as a rather subjective exercise. However, we believe that it gives some general ideas on the reliability of the data presently included in the compilation. Finally, it should be recalled that all the information given in the main data table is anyway provided for users to define

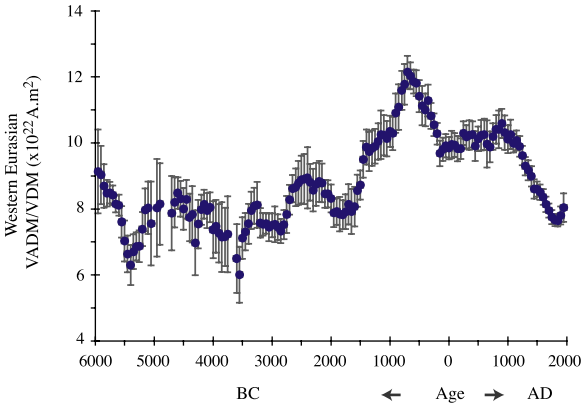

Figure 8. Eight thousand-year-long mixed VADM/VDM variation curve computed for western Eurasia (latitudes $\geq$0 and longitudes comprise between 10°W and 80°E) with the help of sliding windows of 100 years shifted by 50 years. Mean values are reported only when at least three independent results are available per time interval with a data dispersion of less than 20%. The computations are carried out using the selected data discussed in section 5. When data had not originally been corrected for the cooling rate effect, a cooling rate correction of 5% decrease was implemented.

the data selection strategy best suited for their own study.

6. Regional Versus "Global" VADM and VADM/VDM Variation Curves

[44] An interesting question one can discuss with both the present compilation and the sub–data set selected in the way described above is that of the meaning of so-called VADM and mixed VADM/VDM variation curves classically derived whenever enough intensity data are available [e.g., *McElhinny and Senanayake*, 1982; *Yang et al.*, 2000]. This is typically done by converting all intensity data into VADM and VADM/VDM values, which are then used to compute worldwide average values within sliding temporal windows, the hope being that both the geographical and temporal averaging will smooth out most of the nondipole signal (based on, e.g., *Hulot and Le Mouël* [1994]), and that the resulting curve will properly reflect the true slow time changes of the axial (or full) dipole moment. Such a procedure, however, involves a number of potential pitfalls as we shall now illustrate.

[45] The first thing to note is that most of the available data come from western Eurasia. For this reason, we first focus on the region located between longitudes 10°W and 80°E and for latitudes $\geq$0°, which contains $\sim$76% of the data selected. Relying on those data, a rather high resolution VADM/VDM variation curve spanning the past 8 millennia can be computed with the help of sliding intervals of 100 years shifted by 50 years (Figure 8 and Table 1). This was done by implementing an arbitrary but reasonable cooling rate correction of 5% decrease when data had not originally been corrected for the cooling rate effect (Figure 6) [e.g., *Genevey and Gallet*, 2002; *Genevey et al.*, 2003]. We also systematically assigned age uncertainties of 25 years, 50 years, 75 years and 100 years for those results dated from the second millennium A.D., first millennium A.D., first millennium B.C. and beyond when no published age uncertainty was provided, respectively. The derived curve shows large variations with a relatively high mean value over the past four millennia, contrasting with more moderate variations and a lower mean value between 6000 B.C. and 2000 B.C. A prominent peak in intensity is observed during the first half of the first millennium B.C. which *Genevey et al.* [2003] and *Gallet et al.* [2006] already discussed. This peak is followed by two fast decreases during the second half of the first millennium B.C. and the second millennium A.D. which bring the present VADM/VDM estimates back to the level that prevailed some 4000 years ago. It is interesting to plot this curve together with the VADM/VDM variation curve computed in the same way from the selected data for all the rest of the world over just the past three millennia (Figure 9). This reveals significant differences, in particular during the first half of the first millennium A.D. and around the middle of the second millennium A.D. when the curve from "the rest of the world" displays two maxima not seen in the "western Eurasia" curve. This clearly reflects strong contributions from either equatorial dipole or nondipole components which appear not to be averaged out.

[46] The strong geographical bias of the intensity database toward western Eurasia is thus likely to produce erroneous estimates of the global VADM and VADM/VDM values if some care is not taken to properly weight the data as a function of their location, as noted by *Korte and Constable* [2005b]. To illustrate this, we introduced the following simple first-order weighting scheme. We first defined a number of widely distributed geographical regions within which selected data are numerous enough. For the northern hemisphere, 7 such regions of 30° width (both in latitude and longitude) were carefully chosen to avoid any overrepresentation of western Eurasian data (Figure 10a).

Table 1. Western Eurasian VADM and Mixed VADM/VDM Data Computed Over the Past 8 Millennia Using Sliding Windows of 100 Years Shifted by 50 Years[a]

Age	Number of Data	VADM Western Eurasia	VADM Standard Error	Mixed VADM/VDM Western Eurasia	Mixed VADM/VDM Standard Error
6000 B.C.	5	*8.09*	*1.80*	*8.31*	*1.73*
5950 B.C.	5	8.90	1.49	9.13	1.27
5900 B.C.	7	8.91	1.03	9.03	0.89
5850 B.C.	12	8.60	0.72	8.70	0.66
5800 B.C.	16	8.38	0.46	8.48	0.40
5750 B.C.	21	8.41	0.36	8.49	0.33
5700 B.C.	24	8.40	0.30	8.42	0.29
5650 B.C.	20	8.14	0.26	8.15	0.25
5600 B.C.	21	8.14	0.30	8.11	0.32
5550 B.C.	23	7.60	0.47	7.61	0.47
5500 B.C.	16	6.94	0.60	7.03	0.62
5450 B.C.	11	6.40	0.39	6.64	0.55
5400 B.C.	9	6.13	0.44	6.30	0.60
5350 B.C.	10	6.48	0.43	6.70	0.52
5300 B.C.	10	6.67	0.36	6.86	0.43
5250 B.C.	9	6.65	0.40	6.87	0.48
5200 B.C.	10	6.91	0.25	7.39	0.52
5150 B.C.	9	7.38	0.48	7.97	0.65
5100 B.C.	8	7.46	0.60	8.03	0.79
5050 B.C.	6	7.23	1.09	7.56	1.27
5000 B.C.	6	*6.83*	*1.38*	*7.02*	*1.58*
4950 B.C.	4	7.75	1.22	8.04	1.47
4900 B.C.	5	7.78	0.91	8.15	1.24
4850 B.C.	5	7.07	1.20	*7.56*	*1.63*
4800 B.C.	8	6.59	1.11	*7.03*	*1.44*
4750 B.C.	6	6.47	1.27	*7.10*	*1.81*
4700 B.C.	11	7.03	0.80	7.87	1.12
4650 B.C.	16	7.29	0.54	8.20	0.76
4600 B.C.	21	7.59	0.34	8.48	0.48
4550 B.C.	20	7.54	0.38	8.31	0.54
4500 B.C.	17	7.40	0.49	8.00	0.63
4450 B.C.	12	7.63	0.50	8.29	0.59
4400 B.C.	6	7.19	0.58	7.74	0.72
4350 B.C.	6	7.23	0.91	7.84	0.86
4300 B.C.	5	6.31	0.68	6.97	0.98
4250 B.C.	9	6.85	0.76	7.54	0.73
4200 B.C.	13	7.02	0.50	7.98	0.45
4150 B.C.	11	7.14	0.57	8.14	0.44
4100 B.C.	8	6.92	0.57	7.95	0.53
4050 B.C.	10	7.24	0.67	8.05	0.45
4000 B.C.	9	6.97	0.80	7.37	0.86
3950 B.C.	10	7.02	0.72	7.48	0.80
3900 B.C.	9	6.94	0.74	7.26	0.88
3850 B.C.	7	6.78	0.76	7.15	1.06
3800 B.C.	9	6.97	0.76	7.15	0.89
3750 B.C.	6	7.12	1.05	7.23	1.15
3700 B.C.	4	*6.99*	*1.57*	*7.00*	*1.57*
3650 B.C.	4	*6.99*	*1.57*	*7.00*	*1.57*
3600 B.C.	5	6.50	1.04	6.50	1.04
3550 B.C.	3	6.01	0.85	6.01	0.85
3500 B.C.	11	6.99	0.64	7.12	0.63
3450 B.C.	10	7.17	0.59	7.31	0.56
3400 B.C.	13	7.19	0.53	7.55	0.60
3350 B.C.	13	7.45	0.47	7.95	0.57
3300 B.C.	15	7.49	0.40	8.09	0.55
3250 B.C.	8	7.40	0.30	8.12	0.70
3200 B.C.	18	7.14	0.27	7.58	0.45
3150 B.C.	17	7.17	0.25	7.53	0.35
3100 B.C.	15	7.20	0.39	7.56	0.31
3050 B.C.	20	7.14	0.45	7.44	0.42
3000 B.C.	26	7.23	0.37	7.50	0.36
2950 B.C.	18	7.26	0.52	7.53	0.54
2900 B.C.	26	7.19	0.37	7.45	0.39
2850 B.C.	27	7.13	0.37	7.33	0.36
2800 B.C.	30	7.29	0.34	7.52	0.44
2750 B.C.	22	7.54	0.42	7.83	0.56
2700 B.C.	33	7.98	0.35	8.28	0.45
2650 B.C.	33	8.32	0.35	8.62	0.41
2600 B.C.	28	8.40	0.51	8.66	0.57
2550 B.C.	20	8.57	0.63	8.79	0.67
2500 B.C.	19	8.57	0.64	8.89	0.72
2450 B.C.	18	8.56	0.68	8.90	0.76
2400 B.C.	15	8.52	0.79	8.94	0.93
2350 B.C.	11	8.86	0.59	8.81	0.55
2300 B.C.	13	8.50	0.66	8.57	0.64
2250 B.C.	14	8.70	0.66	8.74	0.65
2200 B.C.	17	8.76	0.61	8.83	0.62
2150 B.C.	17	8.70	0.56	8.79	0.58
2100 B.C.	21	8.38	0.39	8.45	0.42
2050 B.C.	21	8.39	0.38	8.46	0.41
2000 B.C.	23	8.25	0.39	8.32	0.42
1950 B.C.	18	7.84	0.40	7.88	0.43
1900 B.C.	29	7.87	0.35	7.92	0.40
1850 B.C.	25	7.75	0.44	7.84	0.53
1800 B.C.	30	7.75	0.36	7.83	0.43
1750 B.C.	25	7.82	0.44	7.92	0.52
1700 B.C.	23	8.04	0.54	8.14	0.61
1650 B.C.	16	7.88	0.64	7.92	0.68
1600 B.C.	18	8.06	0.58	8.07	0.60
1550 B.C.	21	8.54	0.48	8.55	0.49
1500 B.C.	26	8.76	0.44	8.73	0.44
1450 B.C.	30	9.56	0.55	9.50	0.55
1400 B.C.	32	10.00	0.52	9.87	0.53
1350 B.C.	33	9.86	0.59	9.74	0.60
1300 B.C.	34	9.99	0.53	9.84	0.53
1250 B.C.	29	9.99	0.53	9.90	0.53
1200 B.C.	32	10.07	0.56	10.04	0.55
1150 B.C.	25	10.29	0.74	10.25	0.73
1100 B.C.	33	10.20	0.63	10.23	0.61
1050 B.C.	31	10.12	0.55	10.13	0.54
1000 B.C.	43	10.44	0.49	10.35	0.47
950 B.C.	33	10.42	0.52	10.29	0.50
900 B.C.	39	10.92	0.51	10.91	0.59
850 B.C.	36	11.04	0.61	11.09	0.69
800 B.C.	46	11.65	0.57	11.59	0.59
750 B.C.	44	11.85	0.60	11.78	0.62
700 B.C.	52	12.22	0.48	12.14	0.50
650 B.C.	44	12.07	0.40	12.03	0.41
600 B.C.	53	11.98	0.32	11.86	0.36
550 B.C.	47	11.93	0.36	11.81	0.39
500 B.C.	53	11.54	0.46	11.42	0.48
450 B.C.	43	11.18	0.59	11.13	0.60
400 B.C.	60	11.13	0.49	11.00	0.49
350 B.C.	56	11.42	0.48	11.28	0.48
300 B.C.	75	10.95	0.40	10.82	0.39
250 B.C.	59	10.66	0.37	10.55	0.34

Table 1. (continued)

Age	Number of Data	VADM Western Eurasia	Standard Error	Mixed VADM/VDM Western Eurasia	Standard Error
200 B.C.	63	10.35	0.34	10.28	0.33
150 B.C.	43	9.74	0.42	9.68	0.39
100 B.C.	56	9.68	0.34	9.80	0.35
50 B.C.	52	9.76	0.34	9.91	0.35
0	64	9.70	0.31	9.84	0.34
50 A.D.	54	9.80	0.37	9.95	0.42
100 A.D.	69	9.77	0.32	9.93	0.37
150 A.D.	59	9.65	0.34	9.82	0.38
200 A.D.	82	9.62	0.28	9.83	0.31
250 A.D.	67	9.93	0.30	10.30	0.36
300 A.D.	78	9.74	0.29	10.18	0.35
350 A.D.	63	9.85	0.39	10.24	0.45
400 A.D.	71	9.97	0.37	10.25	0.40
450 A.D.	46	9.81	0.42	9.91	0.45
500 A.D.	56	10.01	0.32	10.12	0.37
550 A.D.	46	10.17	0.42	10.23	0.46
600 A.D.	49	10.23	0.42	10.26	0.47
650 A.D.	25	10.09	0.63	9.97	0.71
700 A.D.	37	10.42	0.50	9.88	0.46
750 A.D.	27	10.81	0.49	10.19	0.40
800 A.D.	31	11.10	0.54	10.41	0.43
850 A.D.	23	11.00	0.72	10.41	0.57
900 A.D.	33	11.22	0.53	10.59	0.44
950 A.D.	27	10.64	0.58	10.31	0.52
1000 A.D.	30	10.41	0.48	10.12	0.42
1050 A.D.	21	10.45	0.48	10.26	0.45
1100 A.D.	45	9.75	0.29	9.99	0.28
1150 A.D.	38	9.66	0.30	10.07	0.31
1200 A.D.	43	9.52	0.28	9.89	0.31
1250 A.D.	37	9.40	0.28	9.62	0.29
1300 A.D.	60	9.04	0.26	9.30	0.28
1350 A.D.	55	8.88	0.27	9.17	0.30
1400 A.D.	57	8.71	0.26	8.99	0.31
1450 A.D.	48	8.51	0.27	8.61	0.29
1500 A.D.	77	8.65	0.24	8.60	0.23
1550 A.D.	79	8.66	0.26	8.51	0.23
1600 A.D.	93	8.49	0.26	8.36	0.24
1650 A.D.	98	8.21	0.22	8.14	0.23
1700 A.D.	106	7.98	0.21	7.95	0.21
1750 A.D.	88	7.70	0.21	7.75	0.21
1800 A.D.	91	7.51	0.18	7.67	0.18
1850 A.D.	76	7.45	0.16	7.64	0.17
1900 A.D.	46	7.61	0.26	7.80	0.27
1950 A.D.	25	7.90	0.45	8.04	0.43

[a] Means reported with their standard errors in 10^{22} A.m^2 were derived from the selected sub–data set (see text for further description). Data in italic have a standard error greater than 20% and were not considered in Figure 8.

For the southern hemisphere, only one equivalent region could be defined comprising all archeointensity data from Peru. Altogether these 8 regions group ~95% of the selected data. For each region, we next computed the mean VADM and mixed VADM/VDM curves spanning the past three millennia (whenever possible) using both time intervals of 500 years shifted by 250 years and time intervals of 200 years shifted by 100 years (Figures 10b and 10c, respectively, for the VADM/VDM variations). Mean values were derived only when at least 3 independent results were available per sliding interval with data dispersion of less than 20%. The resulting curves are clearly of different qualities, as can be seen from standard errors (although the data dispersion may reflect nondipole and temporal sampling variations), but some common regional features can be recognized. Common high VADM/VDM values during the first half of the first millennium A.D. are for instance found in the eastern Eurasia, Far East, Pacific and the northwest part of the South America curves which contrasts with lower values seen in curves from the other regions during the same period. Values from the southwest part of the North America and Pacific during the second millennium A.D. are also significantly higher than those obtained from the other regions. Considering the relatively poor quality of most data from the present compilation, it is likely that those regional differences originate both from equatorial dipole and nondipole effects and from erroneous intensity determinations. However, for the sake of the present discussion, we assume intensity errors are reasonably accounted for by the VADM and VADM/VDM error bars.

[47] Starting from those eight regional VADM and VADM/VDM curves, it is then straightforward to

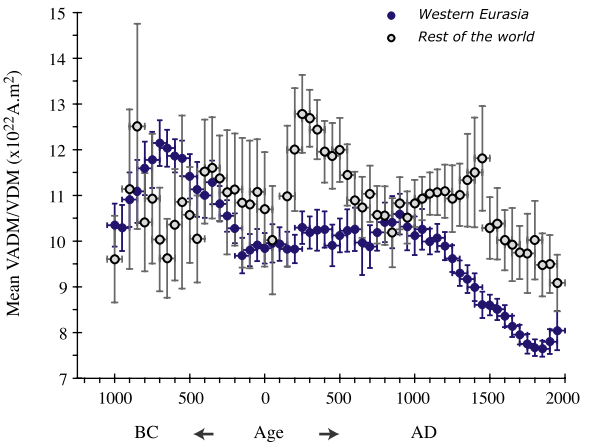

Figure 9. Mixed VADM/VDM variation curves obtained over the past three millennia for western Eurasia (blue dots) and for all the rest of the world (grey dots). Mean values are reported only when at least three independent results are available per time interval with a data dispersion of less than 20%. The computations are carried out using the selected data discussed in section 5. When data had not originally been corrected for the cooling rate effect, a cooling rate correction of 5% decrease was implemented.

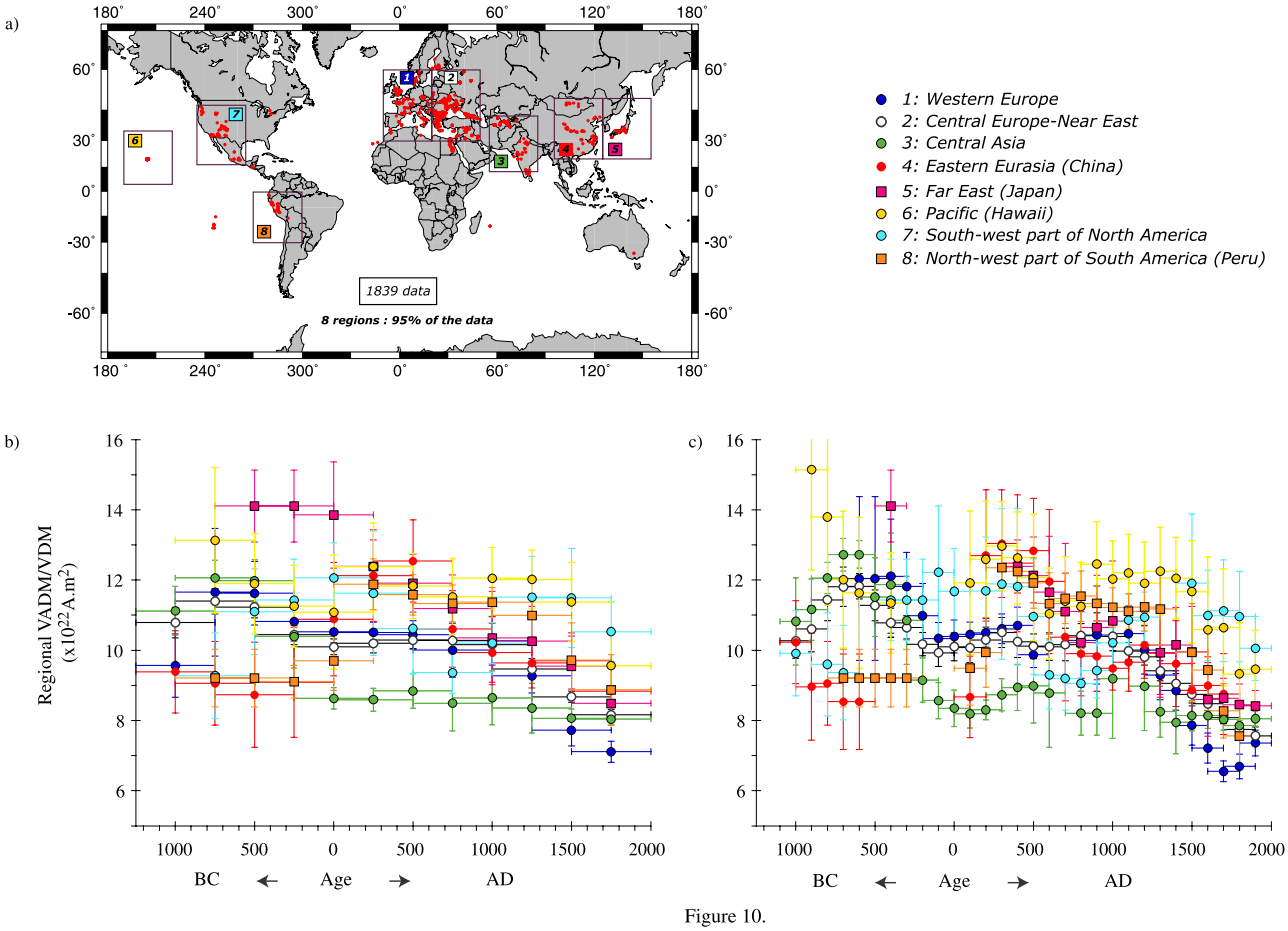

Figure 10.

Figure 10. Geographical distribution of the selected data (red dots) discussed in section 5 and regional mixed VADM/VDM variation curves over the past three millennia. (a) Definition of the eight regions (each 30° width both in latitude and longitude) chosen for the VADM and VDM computations: 1, western Europe (latitudes between 30°N and 60°N, longitudes between 10°W and 20°E); 2, central Europe and Near East (latitudes between 30°N and 60°N, longitudes between 20°E and 50°E); 3, central Asia (latitudes between 12°N and 42°N, longitudes between 55° and 85°E); 4, eastern Eurasia (China; latitudes between 20°N and 50°N, longitudes between 95° and 125°E); 5, Far East (Japan; latitudes between 20°N and 50°N, longitudes between 127°E and 157°E); 6, Pacific (Hawaii; latitudes between 5°N and 35°N, longitudes between 190°E and 220°E); 7, southwest part of North America (latitudes between 17°N and 47°N, longitudes between 235°E and 265° E); 8, northwest part of South America (Peru; latitudes<0°, longitudes between 270°E and 300°E). (b and c) Mixed VADM/VDM regional variation curves (see color code) obtained with the help of sliding windows of 500 years shifted by 250 years and of 200 years shifted by 100 years, respectively. Mean values are reported only when at least three independent results are available per time interval with a data dispersion of less than 20%. When data had not originally been corrected for the cooling rate effect, a cooling rate correction of 5% decrease was implemented.

compute averaged global VADM and VADM/VDM curves (assuming equal weight for each region), which, we may hope, will better reflect dipole field changes. Also it is hoped that the rather long duration of the considered sliding intervals will smooth out some of the remaining nondipole field components [*Hulot and Le Mouël*, 1994] (but see *Constable* [2007, Figure 11]), further reducing possible biases due to the small number of intensity data from the southern hemisphere. Because of the limited number of data outside western Eurasia, such global VADM (Figure 11) and mixed VADM/VDM (Figure 12) curves can be computed only back to the first millennium B.C., the first half of which is clearly less determined (Tables 2 and 3). The curves were in fact computed twice using either all compiled data (grey dots) or only the selected ones (blue dots). The two sets of curves reported in Figures 11 and 12 exhibit the same variations marked by a distinct minimum around the transition between the first millennium B.C. and the first millennium A.D., followed by a

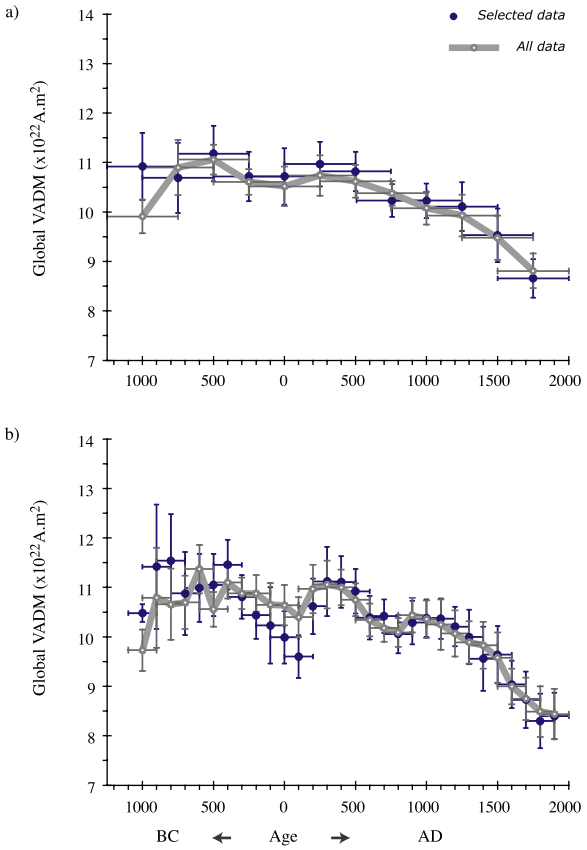

Figure 11. "Global" VADM variation curves over the past three millennia derived from the average of the regional mean values assuming an equal weight for each region. The computations are carried out with the help of sliding windows (a) of 500 years shifted by 250 years and (b) of sliding windows of 200 years shifted by 100 years. Blue dots, selected data; grey dots, all data.

maximum around the third-fourth century A.D. A second minimum is present around the eight century A.D. (Figures 11b and 12b) which is practically smoothed out when the 500-year-long sliding windows are considered (Figures 11a and 12a). In the latter case, a long decrease in VADM and VADM/VDM values is observed over the past ~1750 years. These characteristics are common to all curves, but note that considering all the data generally tends to decrease the amplitude of the observed variations.

[48] We are now in a position to consider the extent to which the regionally weighted estimates of the axial dipole and dipole moment variations differ from more classical estimates derived by combining all data without introducing any regional weighting scheme (white dots, Figure 13). Not surprisingly (recall Figure 10), differences are mainly found within the first half of the first millennium A.D. and the long-term VADM variations from the regionally weighted curve appear to be much smoother (Figure 13a). Comparing our results to the dipole evolution recovered from published spherical harmonic archeomagnetic models, is also of interest [*Hongre et al.*, 1998; *Korte and Constable*, 2005a, 2005b, 2006; *Constable*, 2007]. Large discrepancies are observed between the different curves shown in Figure 14. Considering only the pattern of variations, we note that the dipole moment variation curve computed from regionally averaging the data is similar to the one obtained by *Korte and Constable* [2006] based on the inversion of the directional and intensity data set of *Korte et al.* [2005] for a dipole field only. The same pattern of variations, but with significantly lower dipole moment values, is also found from the CALS7K.2 model of *Korte and Constable* [2005a, 2005b, 2006] based on the inversion of the

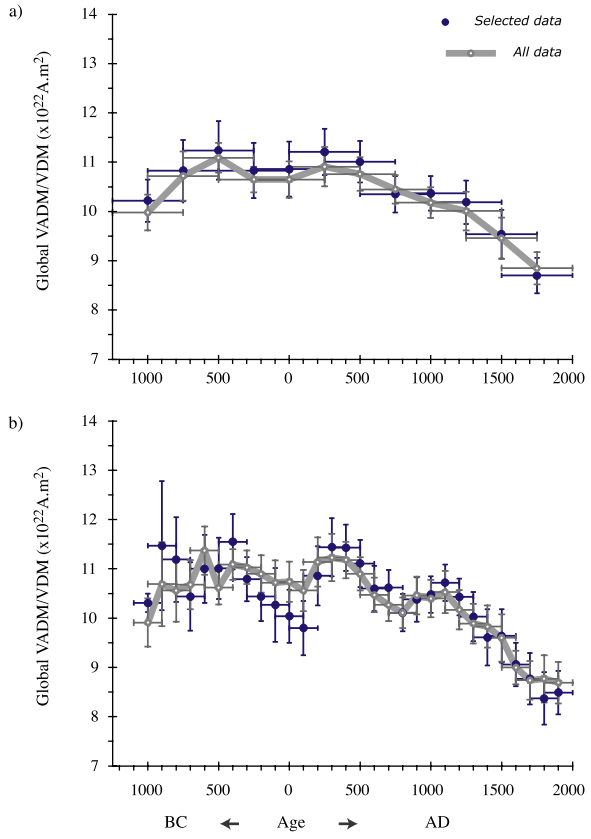

Figure 12. "Global" mixed VADM/VDM variation curves over the past three millennia derived from the average of the regional mean values assuming an equal weight for each region. The computations are carried out with the help of sliding windows (a) of 500 years shifted by 250 years and (b) of sliding windows of 200 years shifted by 100 years. Blue dots, selected data; grey dots, all data.

Table 2. "Global" VADM and Mixed VADM/VDM Data for the Past Three Millennia Computed Using Sliding Windows of 500 Years Shifted by 250 Years and Assuming an Equal Weight for Each Region Defined in the Text[a]

Age	Number of Regions	"Global" VADM	Standard Error	Number of Regions	"Global" Mixed VADM/VDM	Standard Error
1000 B.C.	5	10.92	0.68	4	10.22	0.43
750 B.C.	7	10.69	0.71	7	10.83	0.62
500 B.C.	8	11.18	0.56	8	11.24	0.59
250 B.C.	8	10.72	0.5	8	10.83	0.56
0	8	10.72	0.57	8	10.86	0.56
250 A.D.	8	10.97	0.45	8	11.21	0.47
500 A.D.	8	10.82	0.4	8	11.01	0.42
750 A.D.	8	10.23	0.33	8	10.35	0.37
1000 A.D.	8	10.23	0.35	8	10.37	0.35
1250 A.D.	8	10.11	0.49	8	10.19	0.44
1500 A.D.	8	9.53	0.54	8	9.54	0.49
1750 A.D.	8	8.66	0.39	8	8.7	0.36

[a] Means derived from the selected sub–data set (see text for further description) are reported with their standard errors in 10^{22} A.m^2.

Table 3. "Global" VADM and Mixed VADM/VDM Data for the Past Three Millennia Computed Using Sliding Windows of 200 Years Shifted by 100 Years and Assuming an Equal Weight for Each Region Defined in the Text[a]

Age	Number of Regions	"Global" VADM	Standard Error	Number of Regions	"Global" Mixed VADM/VDM	Standard Error
1000 B.C.	3	10.48	0.18	4	10.31	0.19
900 B.C.	4	11.42	1.26	4	11.47	1.31
800 B.C.	4	11.54	0.94	5	11.19	0.86
700 B.C.	5	10.88	0.84	6	10.44	0.69
600 B.C.	6	10.99	0.69	6	11	0.69
500 B.C.	4	11.05	0.63	4	11.01	0.62
400 B.C.	7	11.46	0.5	7	11.55	0.56
300 B.C.	5	10.81	0.44	5	10.79	0.45
200 B.C.	4	10.44	0.48	4	10.44	0.5
100 B.C.	4	10.23	0.77	4	10.27	0.75
0	5	9.99	0.53	5	10.04	0.54
100 A.D.	6	9.6	0.43	6	9.8	0.55
200 A.D.	7	10.62	0.56	7	10.86	0.6
300 A.D.	6	11.12	0.7	7	11.44	0.59
400 A.D.	7	11.11	0.52	8	11.43	0.47
500 A.D.	8	10.92	0.45	8	11.11	0.48
600 A.D.	7	10.39	0.44	7	10.6	0.46
700 A.D.	6	10.42	0.34	6	10.62	0.36
800 A.D.	8	10.06	0.39	8	10.11	0.38
900 A.D.	8	10.29	0.44	8	10.38	0.45
1000 A.D.	7	10.38	0.38	7	10.48	0.37
1100 A.D.	7	10.37	0.41	6	10.72	0.37
1200 A.D.	8	10.21	0.4	7	10.43	0.37
1300 A.D.	7	10	0.55	7	10.03	0.5
1400 A.D.	6	9.56	0.65	6	9.61	0.57
1500 A.D.	8	9.64	0.58	8	9.64	0.54
1600 A.D.	8	9.04	0.48	8	9.06	0.44
1700 A.D.	8	8.73	0.57	8	8.77	0.52
1800 A.D.	7	8.3	0.55	7	8.37	0.53

[a] Means derived from the selected sub–data set (see text for further description) are reported with their standard errors in 10^{22} A.m^2.

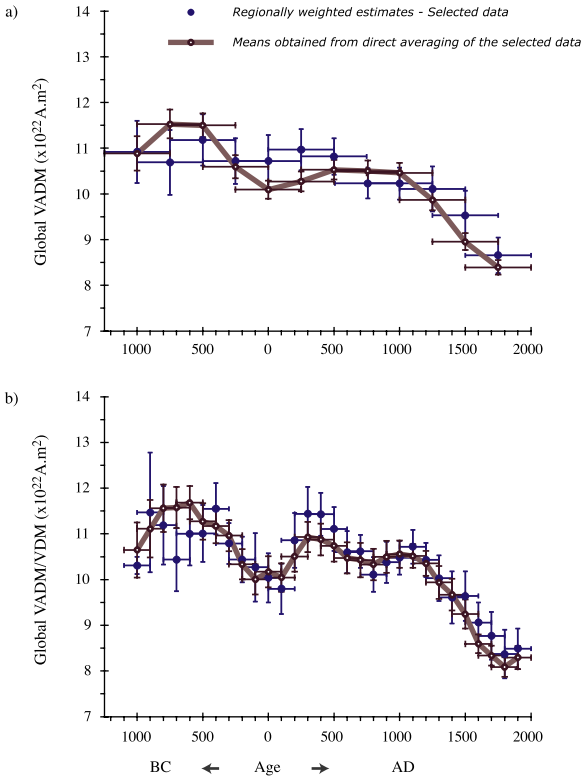

Figure 13. Effect of the geographic bias in the distribution of the available intensity data on the estimates of the (a) "global" VADM and (b) mixed VADM/VDM variation curves. Computations are performed using the selected data smoothed over sliding windows (a) of 500 years shifted by 250 years and (b) of 200 years shifted by 100 years. Blue dots, regionally averaged estimates; brown dots, values obtained from direct averaging of the data.

same *Korte et al.* [2005] data set up to degree 10. Interestingly the earlier model of *Hongre et al.* [1998] based on a much smaller database [*Daly and Le Goff*, 1996], and restricted to dipole and quadrupole terms plus a few octupolar terms because of the poor distribution of the data, appears to provide better numerical agreement (but not in terms of pattern) with our VADM/VDM estimates over the ~600–1700 A.D. time period. The variability among all these estimates can be understood from their distinct implicit parametrizations which partition the intensity variations differently among dipole and nondipole contributions and impose variable temporal resolutions. The temporal resolution of the CALS7K.2 model depends on the data quality at any given time and is difficult to calculate directly, but is certainly no better than the two centuries represented in each of the overlapping block averages in Figure 14. The general smoothness of Hongre et al.'s curve also points to rather low temporal resolution in keeping with the sparse data set. In the interval 300–600 A.D. where the disagreement among the various curves is largest it is possible that an adequate fit to the mainly directional data sets used in CALS7K.2 and by *Hongre et al.* [1998] requires nondipole field contributions which could then perhaps lower the recovered dipole moment compared with the VADM/VDM estimate inferred from the present intensity compilation.

[49] Finally, and relying on the same procedures (i.e., splitting the data set in 8 regions and using a 20% limit for the data dispersion), we also computed estimates of the regionally weighted "global" VADM over the past four centuries. Figure 15 shows that our rough regionally weighting scheme leads to a VADM variation curve with a rather flat evolution between ~1600 A.D. and ~1850 A.D. very comparable to that described by *Gubbins et al.* [2006], who relied on intensity data from *Korte et al.* [2005] powerfully complemented by directional information from the historical model of *Jackson et al.* [2000] thanks to an appropriate uniqueness theorem [*Hulot et al.*, 1997]. For the most recent period, our inferred VADM values also turn out to be compatible with the model of *Jackson et al.* [2000] at times when historical intensity observations were directly available and the historical VADM estimates thus very reliable.

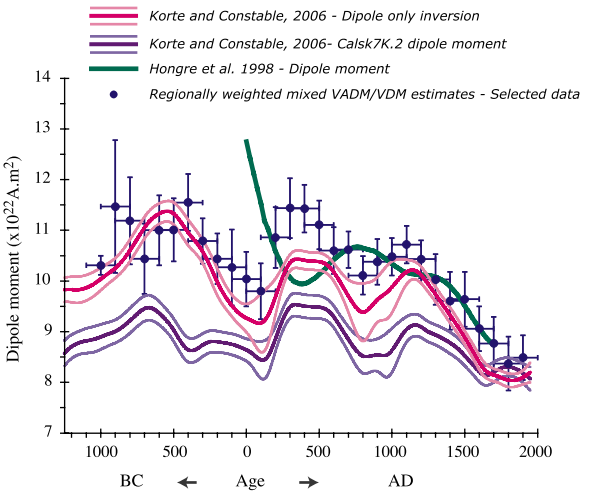

Figure 14. Comparisons between the "global" mixed VADM/VDM variation curve and published dipole moment evolutions. Blue dots: regionally averaged estimates using sliding windows of 200 years shifted by 100 years. The other curves were obtained from the spherical harmonic inversion of both directional and intensity data (green, *Hongre et al.* [1998]; purple, *Korte and Constable* [2005a, 2005b, 2006]; pink, *Constable* [2007]). See the text for further details.

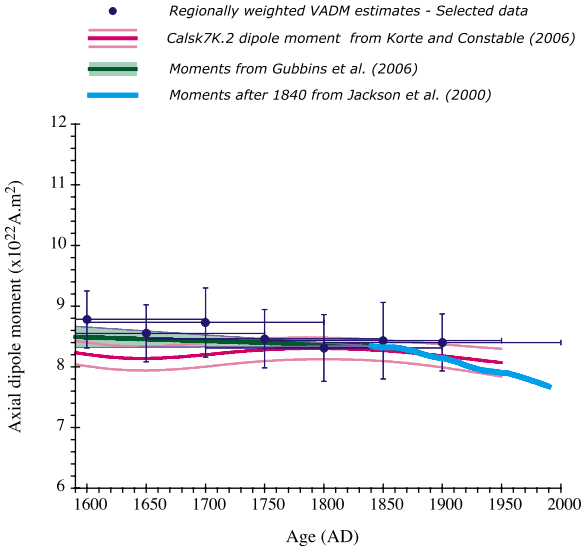

Figure 15. Axial dipole moment evolution over the past four centuries. Blue dots, regionally averaged VADM estimates using sliding windows of 200 years shifted by 50 years. For these computations, we assigned age uncertainties of 25 years and 10 years for those results dated from the [1600–1800] and [1800–2000] age intervals, respectively. Light blue, axial dipole evolution during the 1840–2000 time interval from *Jackson et al.* [2000]; pink, Calsk7K.2 dipole moment evolution during 1590–1950 time interval from *Korte and Constable* [2006]; green, axial dipole evolution during the 1590–1840 time interval computed by *Gubbins et al.* [2006].

[50] As concluding remarks, it appears that computing VADM or VADM/VDM estimates from the present most up-to-date intensity database requires some care. Regional curves can provide interesting regional information, but clearly contain some amount of equatorial dipole and nondipole contributions which make direct interpretations of such curves potentially hazardous. Computing global curves yields more robust information, but this requires at least some regional weighting scheme. The one proposed in this study is rough, but leads to estimates compatible with more sophisticated analysis. The general agreement among all VADM and dipole moment estimates over the historical period is very encouraging, but the overall success of the rough procedure described here should not hide the fact that more sophisticated analyses are clearly needed to recover additional information beyond just the dipole field behavior. It is our hope that the present compilation, which still lacks data from many different regions of the world (in particular in the southern hemisphere) will prompt both new data acquisition and renewed geomagnetic field modeling efforts.

Acknowledgments

[51] We would very much appreciate if the authors of the various publications considered in the present compilation contact us in the event that the information provided about their data happens to need any corrections. The selected sub–data set discussed in the present study will be made available upon request. We are very grateful to Konstantin Burakov, Serafima Burlatskaya, and Inga Nachasova from the Institute of Physics of the Earth (Russia Academy of Sciences) for the fruitful discussions we had together in Moscow about their methodology and their archeointensity data set. We also thank a lot Volodia Pavlov, who warmly welcomed Agnès Genevey during her stay in Moscow. We are also pleased to thank our colleagues who helped us in building this compilation: Annick Chauvin, Ian Hedley, Mimi Hill, Mary Kovacheva, Maxime Le Goff, Martine Paterne, and John Shaw. We further thank Mary Kovacheva and Michael Jackson, who reviewed the manuscript and made helpful comments. This study was partly financed by the INSU-CNRS program "SEDIT" and by NSF EAR-0112290. This is IPGP contribution 2324.

References

Aitken, M. J., P. Alcock, G. Bussel, and C. Shaw (1981), Archaeomagnetic determination of the past geomagnetic intensity using ancient ceramics: Allowance for anisotropy, *Archaeometry*, *23*, 53–64.

Aitken, M. J., A. L. Allsop, G. D. Bussell, and M. B. Winter (1984), Geomagnetic intensity in Egypt and western Asia during the second millennium BC, *Nature*, *310*, 305–306.

Aitken, M. J., A. L. Allsop, G. D. Bussell, and M. B. Winter (1986), Paleointensity determination using the Thellier technique: Reliability criteria, *J. Geomagn. Geoelectr.*, *38*, 1353–1363.

Aitken, M. J., A. L. Allsop, G. D. Bussell, and M. B. Winter (1988a), Determination of the intensity of the Earth's magnetic field during archaeological times: Reliability of the Thellier technique, *Rev. Geophys.*, *26*, 3–12.

Aitken, M. J., A. L. Allsop, G. D. Bussell, and M. B. Winter (1988b), Comment on "The lack of reproducibility in experimentally determined intensities of the Earth's magnetic field," *Rev. Geophys.*, *26*, 23–25.

Aitken, M. J., A. L. Allsop, G. D. Bussell, Y. Liritzis, and M. B. Winter (1989a), Geomagnetic intensity measurements using bricks from Greek churches of the first and second millennia A.D., *Archaeometry*, *31*, 77–87.

Aitken, M. J., A. L. Allsop, G. D. Bussell, and M. B. Winter (1989b), Geomagnetic intensity variation during the last 4000 years, *Phys. Earth Planet. Inter.*, *56*, 49–58.

Aitken, M. J., L. J. Pesonen, and M. Leino (1991), The Thellier palaeointensity technique: Minisamples versus standard size, *J. Geomagn. Geoelectr.*, *43*, 325–331.

Bevington, P. R. (1969), *Data Reduction and Error Analysis for the Physical Sciences*, McGraw-Hill, New York.

Biquand, D. (1994), Effet de la vitesse de refroidissement sur l'intensité de l'aimantation thermorémanente: Etude expérimentale, conséquence théoriques, *Can. J. Earth Sci.*, *31*, 1342–1352.

Burakov, K. S. (1981), Determination of the ancient geomagnetic field in magnetically anisotropic specimens, *Phys. Solid Earth, Engl. Transl.*, *17*, 891–895.

Burakov, K. S., and I. E. Nachasova (1985), Correcting for chemical change during heating in archaeomagnetic determinations of the ancient geomagnetic field intensity, *Phys. Solid Earth, Engl. Transl.*, *21*, 801–803.

Burlatskaya, S. P., I. E. Nachasova, E. J. Didenko, and N. K. Shelestun (1986), Archeomagnetic determinations of geomagnetic field elements, Sov. Geophys. Comm. of the USRR Acad. of Sci., Moscow.

Chauvin, A., Y. Garcia, P. Lanos, and F. Laubenheimer (2000), Paleointensity of the geomagnetic field recovered on archaeomagnetic sites from France, *Phys. Earth Planet. Inter.*, *120*, 111–136.

Coe, R. (1967), The determination of paleointensities of the Earth's magnetic field with emphasis on mechanisms which could cause non-ideal behavior in Thellier's method, *J. Geomagn. Geoelectr.*, *19*, 157–179.

Constable, C. (2007), Centennial- to millennial-scale geomagnetic field variations, in *Treatise on Geophysics*, vol. 5, *Geomagnetism*, edited by M. Kono, pp. 337–372, Elsevier, New York.

Daly, L., and M. Le Goff (1996), An updated and homogeneous world secular variation data base, 1, Smoothing of the archaeomagnetic results, *Phys. Earth Planet. Inter.*, *93*, 159–190.

Dodson, M., and E. McClelland-Brown (1980), Magnetic blocking temperatures of single domain grains during slow cooling, *J. Geophys. Res.*, *85*, 2625–2637.

Donadini, F., K. Korhonen, P. Riisager, and L. J. Pesonen (2006), Database for Holocene geomagnetic intensity information, *Eos Trans. AGU*, *87*(14), 137.

Donadini, F., P. Riisager, K. Korhonen, K. Kahmae, L. Pesonen, and I. Snowball (2007), Holocene geomagnetic paleointensities: A blind test of absolute paleointensity techniques and materials, *Phys. Earth Planet. Inter.*, *161*, 19–35.

Dunlop, D., and Ö. Özdemir (1997), *Rock Magnetism, Fundamentals and Frontiers*, Cambridge Univ. Press, Cambridge, U. K.

Fisher, R. (1953), Dispersion on a sphere, *Proc. R. Soc. London, Ser. A*, *217*, 295–305.

Fox, J., and M. Aitken (1980), Cooling-rate dependence of thermoremanent magnetisation, *Nature*, *283*, 462–463.

Gallet, Y., and M. Le Goff (2006), High-temperature archeointensity measurements from Mesopotamia, *Earth Planet. Sci. Lett.*, *241*, 159–173.

Gallet, Y., A. Genevey, M. Le Goff, F. Fluteau, and S. A. Eshraghi (2006), Possible impact of the Earth's magnetic field on the history of ancient civilizations, *Earth Planet. Sci. Lett.*, *246*, 17–26.

Games, K. P. (1977), The magnitude of the paleomagnetic field: A new non-thermal, non-detrital method using sun-dried bricks, *Geophys. J.R. Astron. Soc.*, *48*, 315–329.

Games, K. P. (1980), The magnitude of the archaeomagnetic field in Egypt between 3000 and 0 BC, *Geophys. J.R. Astron. Soc.*, *63*, 45–56.

Genevey, A., and Y. Gallet (2002), Intensity of the geomagnetic field in western Europe over the past 2000 years: New data from ancient French pottery, *J. Geophys. Res.*, *107*(B11), 2285, doi:10.1029/2001JB000701.

Genevey, A., Y. Gallet, and J. Margueron (2003), Eight thousand years of geomagnetic field intensity variations in the eastern Mediterranean, *J. Geophys. Res.*, *108*(B5), 2228, doi:10.1029/2001JB001612.

Gubbins, D., A. L. Jones, and C. C. Finlay (2006), Fall in Earth's magnetic field is erratic, *Science*, *312*, 900–902.

Halgedhal, S., R. Day, and M. Fuller (1980), The effect of the cooling rate on the intensity of weak field TRM in single domain magnetite, *J. Geophys. Res.*, *85*, 3690–3698.

Hongre, L., G. Hulot, and A. Khokhlov (1998), An analysis of the geomagnetic field over the past 2000 years, *Phys. Earth Planet. Inter.*, *106*, 311–335.

Hulot, G., and J.-L. Le Mouël (1994), A statistical approach to the Earth's main magnetic field, *Phys. Earth Planet. Inter.*, *82*, 167–183.

Hulot, G., A. Khokhlov, and J. L. Le Mouël (1997), Uniqueness of mainly dipolar magnetic fields recovered from directional data, *Geophys. J. Int.*, *129*, 347–354.

Jackson, A., A. Jonkers, and M. Walker (2000), Four centuries of geomagnetic secular variation from historical records, Philos, *Trans. R. Soc. London, Ser. A*, *358*, 957–990.

Kitazawa, K. (1970), Intensity of the geomagnetic field in Japan for the past 10000 years, *J. Geophys. Res.*, *75*, 7403–7411.

Kono, M. (1978), Reliability of paleointensity methods using alternating field demagnetization and anhysteretic remanence, *Geophys. J.R. Astron. Soc.*, *54*, 241–261.

Korte, M., and C. G. Constable (2005a), Continuous geomagnetic field models for the past 7 millennia: 2. CALS7K, *Geochem. Geophys. Geosyst.*, *6*, Q02H16, doi:10.1029/2004GC000801.

Korte, M., and C. G. Constable (2005b), The geomagnetic dipole moment over the last 7000 years: New results from a global model, *Earth Planet Sci. Lett.*, *236*, 348–358.

Korte, M., and C. G. Constable (2006), Centennial to millennial geomagnetic secular variation, *Geophys. J. Int.*, *167*, 43–52, doi:10.1111/j.1365-246X.2006.03088.x.

Korte, M., A. Genevey, C. G. Constable, U. Frank, and E. Schnepp (2005), Continuous geomagnetic field models for the past 7 millennia: 1. A new global data compilation, *Geochem. Geophys. Geosyst.*, *6*, Q02H15, doi:10.1029/2004GC000800.

Kovacheva, M. (1997), Archaeomagnetic database from Bulgaria: The last 8000 years, *Phys. Earth Planet. Inter.*, *102*, 145–151.

Krasa, D., C. Heunemann, R. Leonhardt, and N. Petersen (2003), Experimental procedure to detect multidomain remanence during Thellier-Thellier experiments, *Phys. Chem. Earth*, *28*, 681–687.

Laj, C., C. Kissel, V. Scao, J. Beer, D. M. Thomas, H. Guillou, R. Muscheler, and G. Wagner (2002), Geomagnetic intensity and inclination variations at Hawaii for the past 98 kyr from core SOH-4 (Big Island): A new study and a comparison with existing contemporary data, *Phys. Earth. Planet. Inter.*, *129*, 205–243.

Le Goff, M., and Y. Gallet (2004), A new three-axis vibrating sample magnetometer for continuous high-temperature magnetization measurements: Applications to paleo- and archeointensity determinations, *Earth Planet. Sci. Lett.*, *229*, 31–43.

Leonhardt, R., D. Krasa, and R. S. Coe (2004), Multidomain behavior during Thellier paleointensity experiments: A phenomenological model, *Phys. Earth Planet. Inter.*, *147*, 127–140.

Leonhardt, R., J. Matzka, A. R. L. Nichols, and D. B. Dingwell (2006), Cooling rate correction of paleointensity determination for volcanic glasses by relaxation geospeedometry, *Earth Planet. Sci. Lett.*, *243*, 282–292.

McElhinny, M. W., and W. E. Senanayake (1982), Variations in the geomagnetic dipole: I. The past 50000 years, *J. Geomagn. Geoelectr.*, *34*, 39–51.

Merrill, R., M. McElhinny, and P. McFadden (1996), *The Magnetic Field of the Earth, Paleomagnetism, the Core and the Deep Mantle*, Academic, New York.

Nachasova, I. E., and K. S. Burakov (2000), The geomagnetic field intensity in Central Asia from 6000 to 3000 B.C., *Phys. Solid Earth, Engl. Transl.*, *36*, 358–363.

Néel, L. (1955), Some theoretical aspects of rock magnetism, *Adv. Phys.*, *4*, 191–243.

Papamarinopoulos, S. P. (1987), Geomagnetic intensity measurements from Byzantine vases in the period between 300 and 1650 yr. A.D. (Greece), *J. Geomagn. Geoelectr.*, *39*, 261–270.

Perrin, M., and E. Schnepp (2004), IAGA paleointensity database: Distribution and quality of the data set, *Phys. Earth. Planet. Inter.*, *147*, 255–267.

Riisager, P., and J. Riisager (2001), Detecting multidomain magnetic grains in Thellier paleointensity experiments, *Phys. Earth Planet. Inter.*, *125*, 111–117.

Rogers, J., J. Fox, and M. Aitken (1979), Magnetic anisotropy in ancient pottery, *Nature*, *277*, 644–646.

Rolph, T. C., and J. Shaw (1985), A new method of palaeofield magnitude correction for thermally altered samples and its application to lower carboniferous lavas, *Geophys. J.R. Astron. Soc.*, *80*, 773–781.

Selkin, P. A., and L. Tauxe (2000), Long-term variations in paleointensity, *Philos. Trans. R. Soc. London, Ser. A*, *358*, 1065–1088.

Shaw, J. (1974), A new method of determining the magnitude of the palaeomagnetic field: Application to five historic lavas and five archaeological samples, *Geophys. J.R. Astron. Soc.*, *39*, 133–141.

Tanguy, J. C. (1975), Intensity of the geomagnetic field from recent Italian lavas using a new paleointensity method, *Earth Planet. Sci. Lett.*, *27*, 314–320.

Thellier, E., and O. Thellier (1959), Sur l'intensité du champ magnétique terrestre dans le passé historique et géologique, *Ann. Geophys.*, *15*, 285–376.

Tulloch, A. M. (1992), A study of Recent secular variation of the geomagnetic field as recorded by lavas from Mount Vesuvius and the Canary Islands, Ph.D. thesis, Univ. of Liverpool, Liverpool, U. K.

Valet, J. P., J. Brassart, I. Le Meur, V. Soler, X. Quidelleur, E. Tric, and P. Y. Gillot (1996), Absolute paleointensity and magnetomineralogical changes, *J. Geophys. Res.*, *101*, 25,029–25,044.

Van Zijl, J. S., K. W. T. Graham, and A. L. Hales (1962), The palaeomagnetism of the Stormberg lavas, II. The behaviour of the magnetic field during a reversal, *Geophys. J.R. Astron. Soc.*, *7*, 169–182.

Walton, D. (1984), Re-evaluation of Greek archaeomagnitudes, *Nature*, *310*, 740–743.

Walton, D. (1986), Alteration and its effects on the reproducibility of archaeomagnitudes from Tel-El-Amarna, *J. Geomagn. Geoelectr.*, *38*, 1349–1352.

Walton, D. (1990), The intensity of the geomagnetic field in the eastern Mediterranean between 1600 BC and AD 400, *J. Geomagn. Geoelectr.*, *42*, 929–936.

Walton, D., and H. Balhatchet (1988), Application of a new technique to Greek archaeomagnitudes, *J. Geomagn. Geoelectr.*, *40*, 1503–1510.

Walton, D., J. Share, T. C. Rolph, and J. Shaw (1993), Microwave magnetization, *J. Geomagn. Geoelectr.*, *43*, 333–340.

Wei, Q. Y., W. X. Zhang, D. J. Li, M. J. Aitken, G. D. Bussell, and M. Winter (1987), Geomagnetic intensity as evaluated from ancient Chinese pottery, *Nature*, *328*, 330–333.

Wilson, R. L. (1961), Paleomagnetism in Northern Ireland. Part I, The thermal demagnetization of natural magnetic moments in Rocks, *Geophys. J.R. Astron. Soc.*, *5*, 45–58.

Yang, S., H. Odah, and J. Shaw (2000), Variations in the geomagnetic dipole moment over the last 12000 years, *Geophys. J. Int.*, *140*, 158–162.

Yu, Y., L. Tauxe, and A. Genevey (2004), Toward an optimal geomagnetic field intensity determination technique, *Geochem. Geophys. Geosyst.*, *5*, Q02H07, doi:10.1029/2003GC000630.